



Extreme climate events under global warming in northern Fars Province, southern Iran

Mostafa Naderi¹

Received: 1 February 2019 / Accepted: 24 August 2020 / Published online: 10 September 2020
© Springer-Verlag GmbH Austria, part of Springer Nature 2020

Abstract

The study area, with arid to semi-humid climates, is located in northern Fars Province, southern Iran. Daily precipitation and temperature data from 22 models of the Coupled Model Inter-comparison Project Phase 5 (CMIP5) are used to study climate change for period 2026–2085 under RCP2.6, RCP4.5, and RCP8.5. Daily outputs of each CMIP5 model are downscaled to climatic stations over the study area using LARS-WG tool and transient change factors approach. Daily precipitation is down-scaled to seven climatic stations while daily temperature down-scaled to two stations. Downscaling results indicate that temperature will increase by + 1.85, + 2.5, and + 3.45 °C under the RCP2.6, RCP4.5, and RCP8.5, respectively, while precipitation will reduce by 14, 22, and 20.8%, respectively, within the study area. Standardized precipitation index (SPI) analysis, performed for 3-, 6-, 9-, and 12-month time scales, shows that frequency (duration) of normal periods will increase (decrease) under climate change, however, 12-month SPI analysis shows decreased frequency and increased duration for normal periods. Frequency, duration, severity, and intensity of wet periods may increase, decrease, or not change under climate change, depending on the SPI time scale. The study area will experience more frequent, longer-duration, severed, intensified droughts in the future due to global warming. Extreme storm analysis shows that precipitation depth of most frequent storms (2-year return period storms) will increase, but precipitation depth of less frequent storms (10- and 20-year return period storms) will decrease under climate change. Temperature enhancement, precipitation reduction, and longer-duration, severed, intensified droughts will increase water shortage in the future, resulting in water crisis and reduced security of food production over northern Fars Province.

Keywords Climate change · RCPs · Extreme storm · Wet and dry periods · Northern Fars Province · Iran

1 Introduction

Today, global warming is an obvious phenomenon (Pachauri et al. 2014). Anthropogenic forcing has made a substantial contribution to surface temperature increases since the mid-twentieth century, affected the global water cycle since 1960, contributed to the retreat of glaciers since 1960s, increased surface melting of Greenland ice sheet since 1993, contributed to Arctic sea-ice loss since 1979, and have made a substantial contribution to increases in global upper ocean heat content and to global mean sea level rise observed since 1970s

(Pachauri et al. 2014). Anthropogenic greenhouse gas emissions are mainly driven by population size, economic activity, lifestyle, energy use, land use patterns, technology, and climate policy (Solomon et al. 2007). Climate change studies show that daily precipitation extremes will be intensified due to global warming (O’Gorman 2015). Increased atmospheric water content has a potential to produce higher precipitation amounts, if it is triggered by an external mechanism such as lifting forced by topography (Evans 2010); however, the condensation level of air parcel will shift upward under global warming due to change in temperature lapse rate over lands and oceans (O’Gorman and Schneider 2009; O’Gorman 2015; Siler and Roe 2014; Singh and Goyal 2016).

Droughts, having durations from years to decades, have occurred during the last millennium over, for example, North America, West Africa, and East Asia. Climate models project increased aridity in the twenty-first century over most of Africa, southern Europe, Middle East, most of the Americas, Australia, and Southeast Asia (Dai 2011). Wet

✉ Mostafa Naderi
m.naderi@iasbs.ac.ir; naderi64@gmail.com

¹ Department of Earth Sciences, Institute for Advanced Studies in Basic Sciences (IASBS), Zanjan, Iran

and dry periods may be monitored by their frequency, duration, severity, and intensity (Jiang et al. 2015). Analysis of shorter-duration droughts may be important to agricultural interests, while longer-duration droughts covering multiple years may be important for water management applications (Swain and Hayhoe 2015). Raje and Mujumdar (2010) concluded that probability of extreme, severe and moderate droughts will increase but probability of normal and wet conditions in Orissa, India, will decrease as a result of climate change. Climate change study over California showed that frequency of dry days, very-heavy precipitation days, and wet and dry periods will increase under climate change (Berg and Hall 2015). Storms control effective groundwater recharge, reservoir storage, soil erosion, and risk of flooding in a given region. The intensified storms increase risk of flooding and soil erosion, may lead to dam failure and change in effective groundwater recharge.

Nowadays, the General Circulation Models (GCMs) are state-of-the-art tools to study the future climate response to global warming in horizontal coarse resolutions of about 250 to 600 km (Task Group on Data Scenario Support for Impact and Climate Analysis TGICA 2007; Green et al. 2011). Climate response is influenced by both regional and local conditions in a region. Local factors such as topography, vegetation, soil characteristics, and local moisture affect the climate of a region. The GCMs simulate well the regional climate responses, but they are weak in simulating the local climate responses due to coarse spatial resolutions. Downscaling techniques have been developed to modify GCM outputs from coarse resolutions to finer resolutions. Among the developed downscaling techniques, the statistical downscaling methods can modify GCM outputs to resolutions even in a single meteorological station (Wilby et al. 2004).

Climate characteristics of a region such as average annual precipitation and temperature, intensity of storms and duration of droughts, and wet years are main climatic factors which directly affect the water resources, and change in these factors due to climate change will alter water availability in the region (Lee et al. 2006; Scibek et al. 2007; Woldeamlak et al. 2007; Aguilera and Murillo 2009; Candela et al. 2009; Wada et al. 2010; Ali et al. 2012; Kabiri et al. 2015; Naderi and Raeisi 2016; Naderi 2020). Therefore, climate change study in a region is useful as a primary material for future sustainable water resource management (Mall et al. 2006; Loáiciga 2009). Towards this issue, many studies have assessed the impact of climate change on precipitation, temperature, and extreme weather events over Iran (Table 1). They may be categorized based on the number of GCMs used for climate change analysis, type and number of scenarios, and size of the study area. Most studies used less than 6 GCMs (Ahmadebrahimpour et al. 2019; Babaeian et al. 2015; Bannayan and Rezaei 2014; Etemadi et al. 2016; Fakhri et al. 2012; Mirdashtvan

et al. 2018; Modarres et al. 2018; Motiee et al. 2019; Roshan et al. 2013; Vaghefi et al. 2019); however, some researchers used 10–20 GCMs for climate change study (Fadia Maghsood et al. 2019; Gohari et al. 2013; Karandish et al. 2017; Rahmani and Zarghami 2013). Climate change is studied under both old scenarios (B1, B2, A1B, A2) and new scenarios (RCP2.6, RCP4.5, RCP8.5), and size of the study area varies from city to national scale. Climate change studies over different parts of the country indicate, in summary, that all regions will warm in the future; however, temperature enhancement depends on the geographical location and type of GCM and scenario. Despite the positive anomaly for temperature, the response of mean annual precipitation to climate change differs among regions. The precipitation may increase and/or decrease in the future, depending on the region and type of GCM and scenario. These studies also reveal that the frequency and precipitation depth of extreme storms and frequency and duration of droughts will increase under climate change in different parts of the country (Ahmadebrahimpour et al. 2019; Modarres et al. 2018; Vaghefi et al. 2019).

Beside the previous valuable studies, this paper has focused on northern parts of Fars Province in southern Iran (Fig. 1). Climate varies from arid to semi-humid and elevation from 320 to 4250 m above sea level (m.a.s.l.). The mean annual precipitation varies from 140 to 677 mm and originates from three different regions of the Mediterranean Sea, Red Sea, and Indian Ocean (Alijani and Harman 1985; Beyglou et al. 2009; Parab Consulting Engineers 1996; Roshani et al. 2013).

There are large dams of Dorudzan and Mollasadra and under-construction dams of Parsian and Sheshpir within the study area to supply the agricultural and municipal water demands. The study of temporal variability of observed precipitation and temperature in southern Iran showed that the precipitation and temperature trends are negative and positive, respectively (Kousari and Zarch 2011; Tabari and Talaee 2011). Climate change may intensify water crisis in this region and make water management difficult in the future. The knowledge of precipitation and temperature change, drought durations, and frequency of extreme storms are vital prerequisites for sustainable water allocation in the future. Also, in the aspect of agricultural activities, it should be note that total cultivated area (7130 km²) in Fars Province contributes to 6.1% of the country's cultivated area (117,664 km²). About 15 and 8.1% of garden and crop products over the country is due to the Fars Province, leading to first and second rank of garden and crop productions, respectively, among the provinces (Fars Agriculture Organization 2017). Dominant garden crops are citrus, grape, pomegranate, apple, and olive, and dominant farm crops are wheat, barley, alfalfa, and corn (Fars Agriculture Organization 2017).

Cultivated areas are reduced during droughts due to limited available water resources in recent decade. The reduction of food production under climate change in the study area will

Table 1 Climate change studies in Iran and study area

Researcher(s)	Number of GCM(s)	Scenario(s)	Region's size	Contain the study area?	Results
Bannayan and Rezaei (2014)	2	B1, A1B, A2	Province	No	Mean annual precipitation will decrease in Khorasan province under 3 scenarios.
Fakhri et al. (2012)	6	A1, A2, B1, B2	City	No	Precipitation in Shahr-e Kord city approximately increases between 100 and 500 mm in the future period.
Etemadi et al. (2016)	2	A1B	Province	No	Winter precipitation in Hormozgan province decreases while summer precipitation increases during the period 2080–2099.
Rahmani and Zarghami (2013)	15	B1, A1B, A2	Regional	No	Annual temperature in northwestern provinces of Iran increases up to 4.5 °C. Precipitation is expected to increase in summer and fall while changes in wintry precipitation depend on the location.
Roshan et al. (2013)	1	A1	Regional	No	Precipitation change from – 51 to +93 mm in northwestern Iran depends on the location. The risk of flooding increases under climate change.
Gohari et al. (2013)	10	B1, A2	Basin	No	The temperature will increase by 1.1–1.5 °C in Zayandeh-Rud river basin and precipitation decrease by 11–30% under climate change.
Babaeian et al. (2015)	1	B2, A2	National	Yes	Iran will experience a temperature increase by 3–5.5 °C during the period of 2071–2100 and precipitation reduction by 7.8–10.1 mm. The precipitation over the study area will decrease by 35% and temperature raise by about 3.5–5 °C
Karandish et al. (2017)	15	B1, A1B, A2	National	Yes	Climate change projections show increase of the average annual precipitation at the national level under A1B, A2, and B2 scenarios with a range of 8.14–21.86%. The precipitation and temperature in the study area will increase by 10% and 1 °C, respectively.
Modarres et al. (2018)	6	B1, A2	Regional	No	The frequency of extreme storms will increase in northern Iran due to climate change.
Vaghefi et al. (2019)	5	RCP4.5, RCP8.5	National	Yes	Iran, especially southern parts, will likely experience more extended dry conditions and higher frequency of floods. There is no selected station in the study area and results are interpolated using the surrounding stations. Precipitation decrease by 25 mm, frequency of dry periods and floods will increase in the study area.
Fadia Maghsood et al. (2019)	20	RCP2.6, RCP8.5	Basin	No	The precipitation, temperature, and risk of flooding in Talar river watershed, northern Iran, will increase.
Ahmadebrahimpour et al. (2019)	1	RCP2.6, RCP8.5	Basin	No	The frequency and duration of droughts over watershed of Urmia Lake will increase.
Mirdashtvan et al. (2018)	1	RCP2.6, RCP4.5, RCP8.5	Basin	No	The annual precipitation decrease and temperature increase over the watershed of Karaj and Jajrud rivers in Tehran province.
Motiee et al. (2019)	5	RCP4.5, RCP8.5	Basin	No	The precipitation in Sardabrud river, Alam-Kuh glacier in northern Iran, decreases by 6% and temperature increases by 1 °C during the future period of 2021–2040.

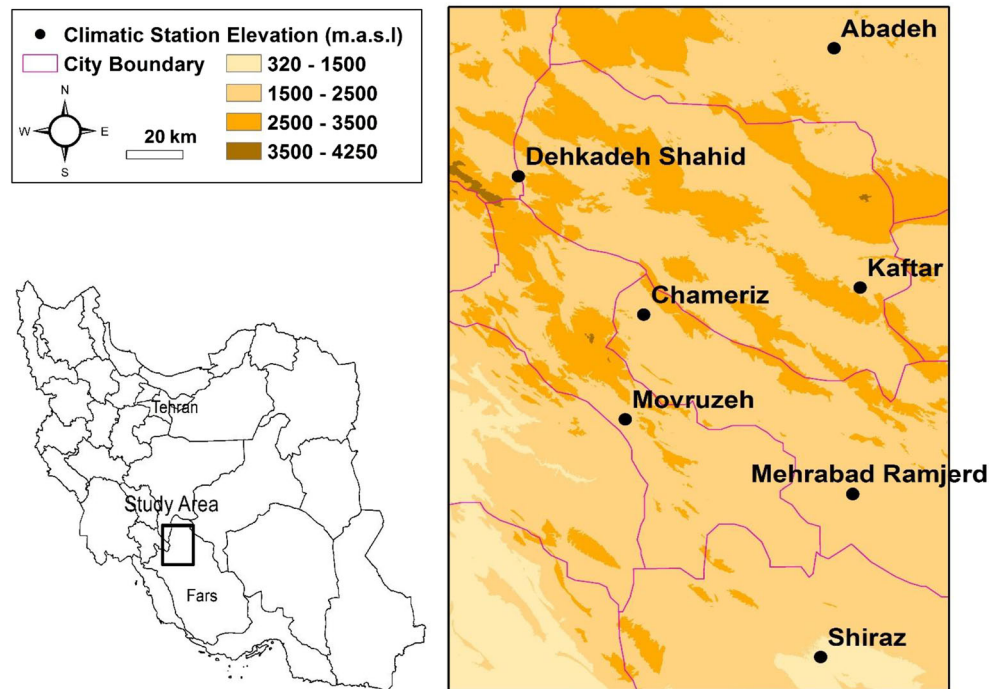
affect the security of food in the province and country. The groundwater table has been declined in recent two decades either due to frequent severe droughts or groundwater over-exploitation over the study area. A vital issue for future sustainable water resource management and food production in northern Fars Province is to address the available water, duration of wet years and droughts, and frequency of extreme storms under climate change. Therefore, the aim of this study is to assess the impact of climate change (future 60-year period) on precipitation, temperature, frequency, duration, severity, and intensity of wet years and droughts, and precipitation

depth of extreme storms in northern Fars Province of southern Iran.

2 Study area

The study area is located in northern Fars Province, southern Iran. It extends within an area of about 28,775 km² (Fig. 1). Climate varies from arid to semi-humid based on the De Martonne Index (De Martonne 1926) (Table 2). Elevation varies from 320 m.a.s.l. in southwest of the region to

Fig. 1 The study area and location of seven climatic stations



4250 m.a.s.l. at higher latitudes (Zagros Mountains). Elevation ranges of 320–1500, 1500–2500, 2500–3500, and 3500–4250 m.a.s.l. cover about 8.8, 70.9, 20, and 0.3% of the study area, respectively. Therefore, dominant topography ranges from 1500 to 2500 m.a.s.l. (Fig. 1).

The precipitation regime has been studied by Alijani and Harman (1985), Parab Consulting Engineers (1996), Beyglou et al. (2009), and Roshani et al. (2013) in southern Iran. They found that three regions including the Mediterranean Sea, Red Sea, and Indian Ocean contribute to precipitation by 74, 23, and 3%, respectively. The Mediterranean and Red Sea air masses come from northwest and southwest parts of the study area, respectively, and Indian Ocean monsoons from southeast. Annual precipitation significantly varies from 140 mm in

northeast to 677 mm in west and southwest of the study area (Table 2). Water resources have been continually depleted due to the frequent droughts and over-exploitation of water resources, while climate change may intensify water crisis in the future.

3 Methodology

3.1 Measured data

Seven climatic stations are selected based on the longest common daily records of precipitation and temperature data to assess climate change in the study area (Fig. 1). Daily

Table 2 The mean annual temperature (T), precipitation (P), and climate of seven stations in the study area

Station	Elevation (m)	T ($^{\circ}\text{C}$)	P (mm)	De Martonne Index	Climate
Abadeh	2030	14.3	140	5.76	Arid
Chameriz	1810	14.8	495	19.96	Semi-arid to Mediterranean
Dehkadeh Shahid	2256	15*	507	20.28	Mediterranean
Kaftar	2342	11.9	508	23.19	Mediterranean
Mehrabad Ramjerd	1606	15.4	384	15.12	Semi-arid
Movruzeh	1946	15*	677	27	Semi-humid
Shiraz	1484	18.3	346	12.22	Semi-arid

*The value is estimated from nearest station

Table 3 Available, included, and excluded general circulation models (GCMs) for the study area under the three RCPs

GCM number	RCP2.6	RCP4.5	RCP8.5
1	–	<i>ACCESS1.0</i> ^a	<i>ACCESS1.0</i> *
2	–	<i>ACCESS1.3</i> *	<i>ACCESS1.3</i> *
3	–	<i>CCSM4</i> *	<i>CCSM4</i> *
4	–	–	<i>CMCC-CESM</i> *
5	–	<i>CMCC-CM</i> *	<i>CMCC-CM</i> *
6	–	<i>CMCC-CMS</i> *	<i>CMCC-CMS</i> *
7	<i>CNRM-CM5</i> *	<i>CNRM-CM5</i> *	<i>CNRM-CM5</i> *
8	<i>CSIRO-Mk3.6.0</i> *	<i>CSIRO-Mk3.6.0</i> *	<i>CSIRO-Mk3.6.0</i> *
9	–	CSIRO-Mk3L-1-2	–
10	–	EC-EARTH	EC-EARTH
11	FGOALS-g2	FGOALS-g2	FGOALS-g2
12	–	FGOALS-s2	FGOALS-s2
13	GFDL-CM3	GFDL-CM3	GFDL-CM3
14	GFDL-ESM2G	GFDL-ESM2G	GFDL-ESM2G
15	–	<i>GISS-E2-H</i> *	<i>GISS-E2-H</i> *
16	–	<i>GISS-E2-R</i> *	<i>GISS-E2-R</i> *
17	–	HadCM3	–
18	<i>HadGEM2-AO</i> *	<i>HadGEM2-AO</i> *	<i>HadGEM2-AO</i> *
19	–	HadGEM2-CC	HadGEM2-CC
20	<i>HadGEM2-ES</i> *	<i>HadGEM2-ES</i> *	<i>HadGEM2-ES</i> *
21	–	<i>INM-CM4</i> *	<i>INM-CM4</i> *
22	<i>IPSL-CM5A-LR</i> *	<i>IPSL-CM5A-LR</i> *	<i>IPSL-CM5A-LR</i> *
23	<i>IPSL-CM5A-MR</i> *	<i>IPSL-CM5A-MR</i> *	<i>IPSL-CM5A-MR</i> *
24	–	<i>IPSL-CM5B-LR</i> *	<i>IPSL-CM5B-LR</i> *
25	<i>MIROC-ESM</i> *	<i>MIROC-ESM</i> *	<i>MIROC-ESM</i> *
26	<i>MIROC-ESM-CHEM</i> *	<i>MIROC-ESM-CHEM</i> *	<i>MIROC-ESM-CHEM</i> *
27	–	MIROC4h	–
28	MIROC5	MIROC5	MIROC5
29	<i>MPI-ESM-LR</i> *	<i>MPI-ESM-LR</i> *	<i>MPI-ESM-LR</i> *
30	<i>MPI-ESM-MR</i> *	<i>MPI-ESM-MR</i> *	<i>MPI-ESM-MR</i> *
31	<i>MRI-CGCM3</i> *	<i>MRI-CGCM3</i> *	<i>MRI-CGCM3</i> *
32	–	–	MRI-ESM1
33	<i>Nor-ESM1-M</i> *	<i>Nor-ESM1-M</i> *	<i>Nor-ESM1-M</i> *
Number of included models	12	21	22
Number of excluded models	4	10	8

*Included GCMs

precipitation is recorded in seven stations since 1978. Temperature is recorded in five stations, but daily minimum and maximum temperature data are recorded only in Abadeh and Shiraz stations since 1978 (Table 2). Therefore, precipitation is downscaled to seven stations, but temperature is downscaled to Abadeh and Shiraz stations.

3.2 GCMs and scenarios

Projection of climate variables under global warming, especially for precipitation, using different GCMs include

considerable uncertainty (Senior and Mitchell 1993; Reichler and Kim 2008; Mandal et al. 2016). The uncertainty in projection of climate variables is mainly due to difference in GCM’s spatial resolution, parameterization, and adjusting fluxes of heat, momentum, and freshwater (Senior and Mitchell 1993; Reichler and Kim 2008; Mandal et al. 2016). Therefore, in this study, daily outputs from 22 models of the CMIP5 are applied for climate change study to incorporate the uncertainty in temperature and precipitation projections using different GCMs (Table 3). Daily outputs of CMIP5 models under RCPs are available through <https://esgf-data.dkrz.de/>

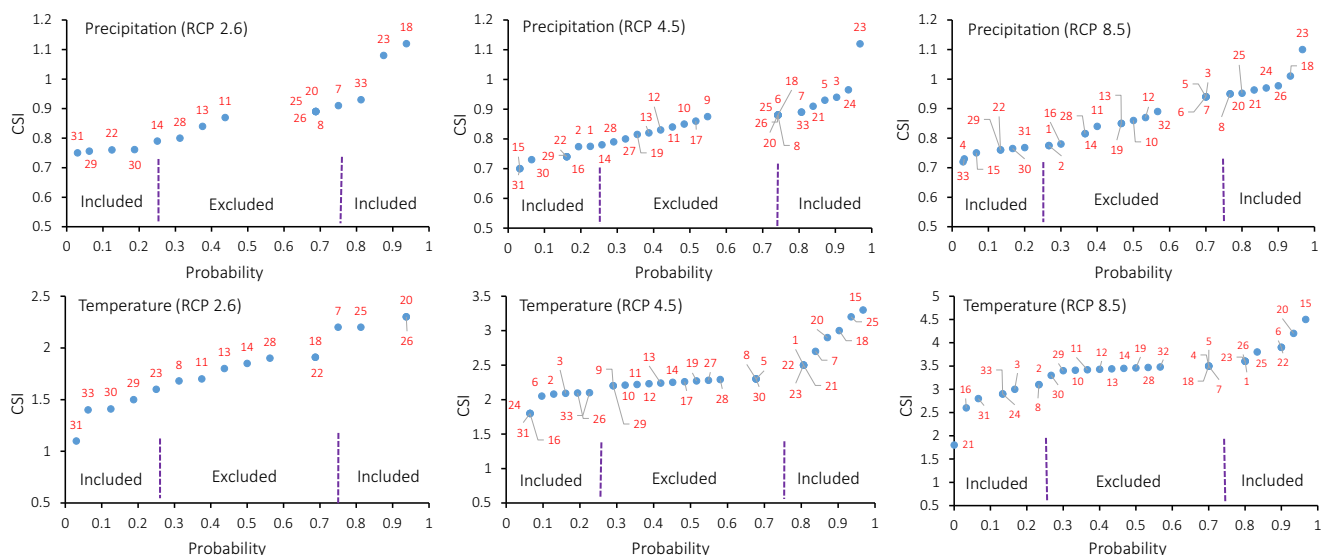


Fig. 2 Probability distribution of precipitation and temperature climate sensitivity indices (CSI) for available CMIP5 models. Numbers denote the related number of the general circulation models (GCM) listed in Table 3

search/cmip5-dkrz (World Climate Research Programme 2018). The CMIP5 provides outputs of more than one GCM from an individual institution or more than one version of a given GCM (Ho et al. 2016; Thompson et al. 2017), leading to model- and institution-dependent results for climate change studies (Ho et al. 2016; Knutti and Sedláček 2013; Thompson et al. 2017). Potential for such biases to influence the ensemble mean can be addressed using the climate sensitivity indices approach (Naderi and Saatsaz 2019; Semenov and Stratonovitch 2015).

The available GCMs, regardless of version and institution, were 16, 31, and 30 models for the RCP2.6, RCP4.5, and RCP 8.5, respectively (Table 3). The method of climate sensitivity indices (CSI) proposed by Semenov and Stratonovitch (2015) was used to select a subset of GCMs while it preserves the range of uncertainty that exists in the CMIP5 models and eliminates model-dependent biases. The CSI for precipitation (temperature) is defined as the spatial-averaged, calculated over a region, relative change (difference) between mean values for the future and baseline periods of a given GCM. Then, 25th (limit of lowest values) and 75th (limit of highest values) CSI percentiles were selected to include GCMs in climate change study (Naderi and Saatsaz 2019), see Fig. 2 and Table 3. Included GCMs are 12, 21, and 22 models for the RCP2.6, RCP4.5, and RCP 8.5, respectively (Fig. 2; Table 3).

Different alternatives of driven factors are considered in twenty-first century to project the greenhouse gasses in Representative Concentration Pathways (RCP) scenarios. The RCPs describe different pathways of greenhouse gas emissions, air pollutant emissions, and land use. Climate change for period 2026–2085 is studied under the three

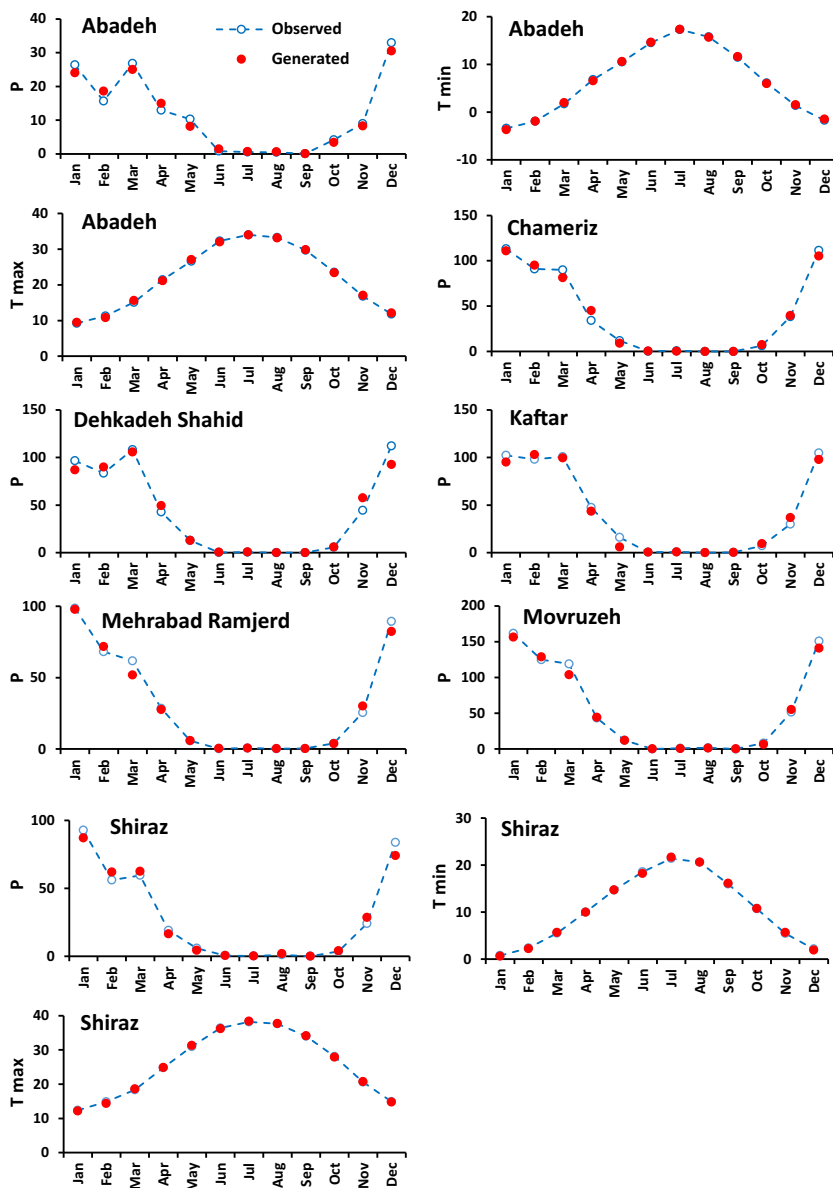
RCPs including: RCP2.6, RCP4.5, and RCP8.5. The RCP2.6 is a stringent mitigation scenario, RCP4.5 an intermediate global warming scenario, and RCP8.5 a very high greenhouse gas emission scenario whose radiative forcings are + 2.6, + 4.5, and + 8.5 W/m^2 , respectively in the year 2100 relative to pre-industrial values (Pachauri et al. 2014).

3.3 Downscaling

Statistical downscaling is modification of GCM outputs from a coarse resolution to a finer resolution, even at a single climatic station. In this study, the Long Ashton Research Station Weather Generator (LARS-WG) is used to downscale each GCM-predicted data to seven climatic stations. The LARS-WG performs well in different climates to reproduce climate variables statistically similar to the observed climate in a region (Semenov et al. 1998; Semenov and Stratonovitch 2010). The LARS-WG has a standard procedure to downscale GCM daily outputs to a single climatic station. The procedure contains three steps of calibration, verification, and generation under the influence of change factors (Semenov and Barrow 2002; Semenov 2007).

Observed daily data for period 1978–2005 (28-year period) are inputted to the LARS-WG to calibrate it for each station. Then, to verify the model, 28-year daily data are generated. The Kolmogorov–Smirnov (K-S) test at significance level of 0.01 is applied to compare generated seasonal statistical distributions of wet and dry series, monthly statistical distributions of precipitation, and minimum and maximum temperature with observed distributions (Semenov and Barrow 2002; Iizumi et al. 2012). The mean monthly precipitation and minimum and maximum temperature are compared using the Student's *t* test

Fig. 3 Comparison between generated and observed mean monthly precipitation and minimum and maximum temperature at seven climatic stations during the observation period 1978–2005



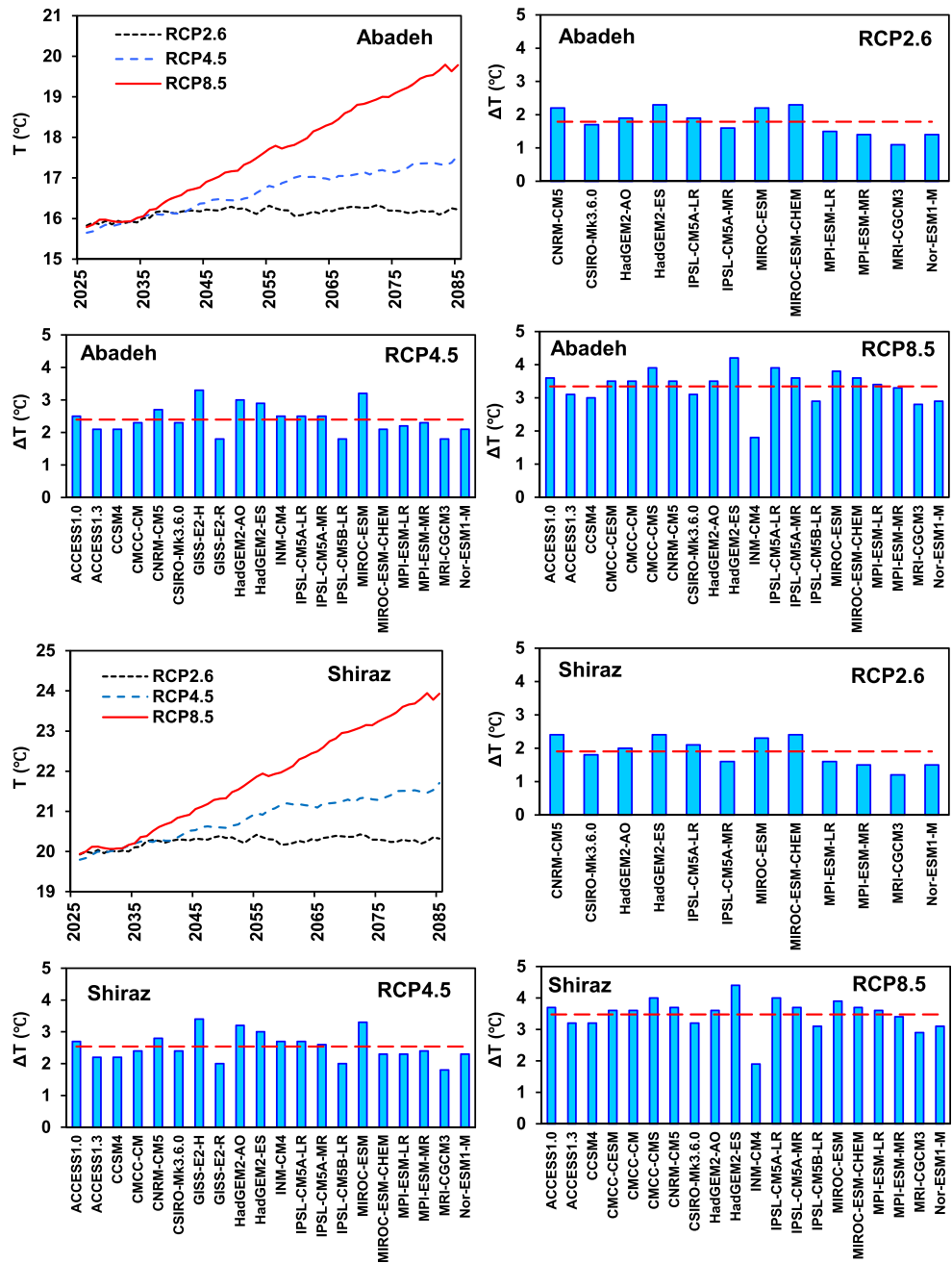
at significance level of 0.01 (Semenov and Barrow 2002; Iizumi et al. 2012). Comparison between generated and observed mean monthly precipitation and minimum and maximum temperature data during the observation period 1978–2005 (Fig. 3) implies that the LARS-WG reproduces precipitation and temperature data well in seven climatic stations. Daily precipitation is generated using serial approach (Racsko et al. 1991; Semenov and Barrow 2002). The probability distributions of precipitation and lengths of wet and dry spells are calculated for each month, and then, a semi-empirical exponential function is fit to these data. The semi-empirical distributions give flexibility to the LARW-WG, allowing it to model a wide variety of distributions (Semenov 2007). The LARS-WG generates minimum and maximum daily temperature

using normalization method (Racsko et al. 1991) where semi-empirical exponential functions are fit to observed normalized data for each month. The LARS-WG also uses

Table 4 The original SPI classification (McKee et al. 1993)

SPI	Category
≥ 2	Extremely wet
1.5–1.99	Very wet
1–1.49	Moderately wet
–0.99 to 0.99	Near normal
–1 to –1.49	Moderately dry
–1.5 to –1.99	Severely dry
≤ -2	Extremely dry

Fig. 4 Downscaled annual temperature (T) to Abadeh and Shiraz stations using the CMIP5 ensemble and predicted change in mean annual temperature (ΔT) for the period 2026–2085 relative to baseline period (1978–2005) under different CMIP5 models and RCPs. Dashed line shows mean value



random seed for random probability generation of wet and dry spell lengths, daily precipitation, and minimum and maximum temperature, allowing the user to change the random seed until being able to achieve acceptable verification results (Semenov and Barrow 2002).

Third step (downscaling) requires calculating monthly change factors for the parameters of precipitation depth, wet and dry spell length, standard deviation of mean temperature, and minimum and maximum temperature. Change factors must be calculated for each climatic station using the given GCM and relevant grid. Change

factors of precipitation depth, wet and dry spell lengths, and standard deviation of mean temperature are defined as ratio of corresponding values in the future period to calibration period. Change factors of minimum and maximum temperature are the difference between corresponding values in the future and calibration periods.

Naderi and Raeisi (2016) used a 1-year shifting forward procedure to calculate change factors transiently in which future time window was selected as 5 years. They demonstrated that the 5-year time window is suitable to study climate change, especially in assessing the impact

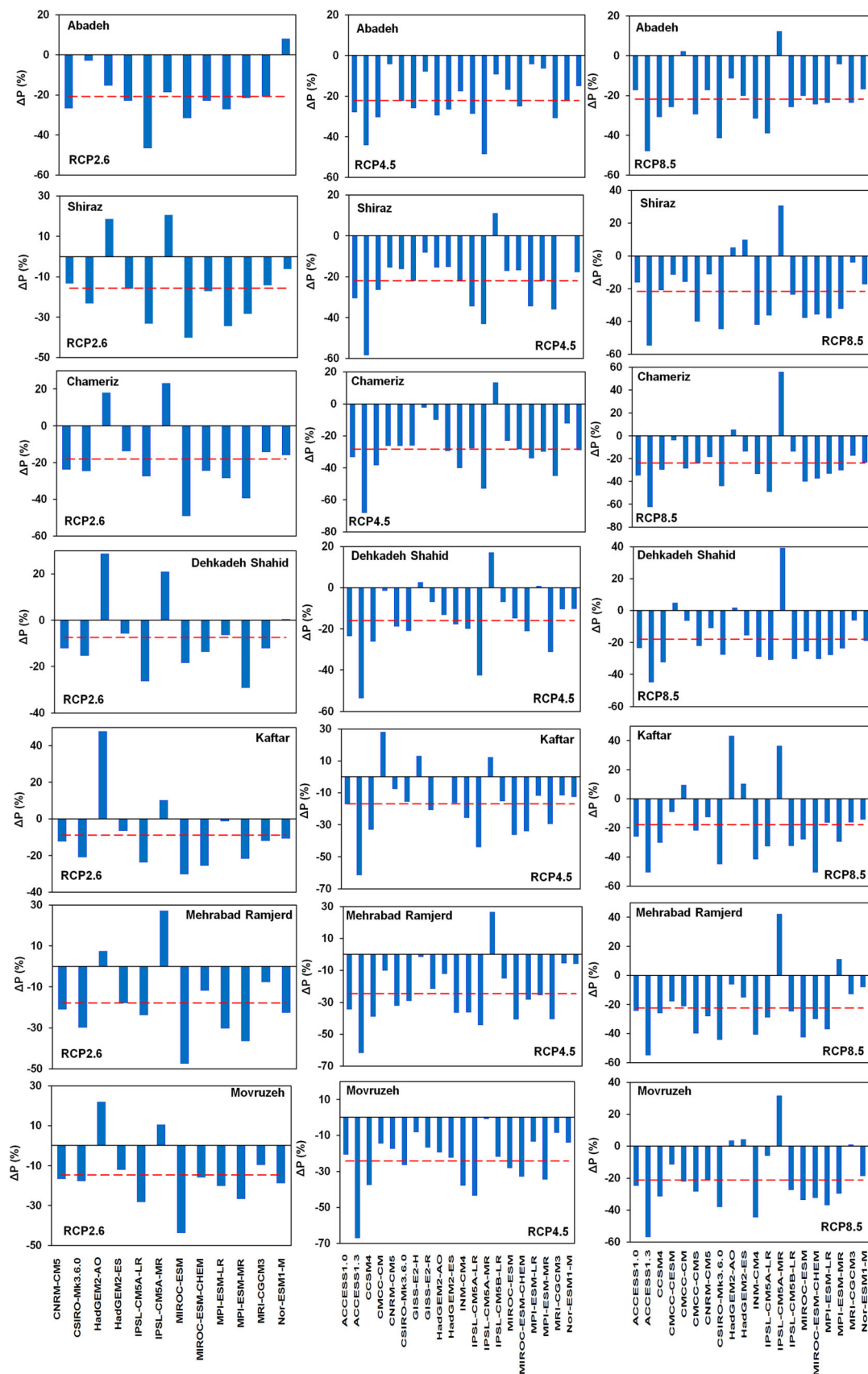


Fig. 5 The predicted change in mean annual precipitation (ΔP) for the period 2026–2085 relative to baseline period (1978–2005) under different CMIP5 models and RCPs. Dashed line shows mean value

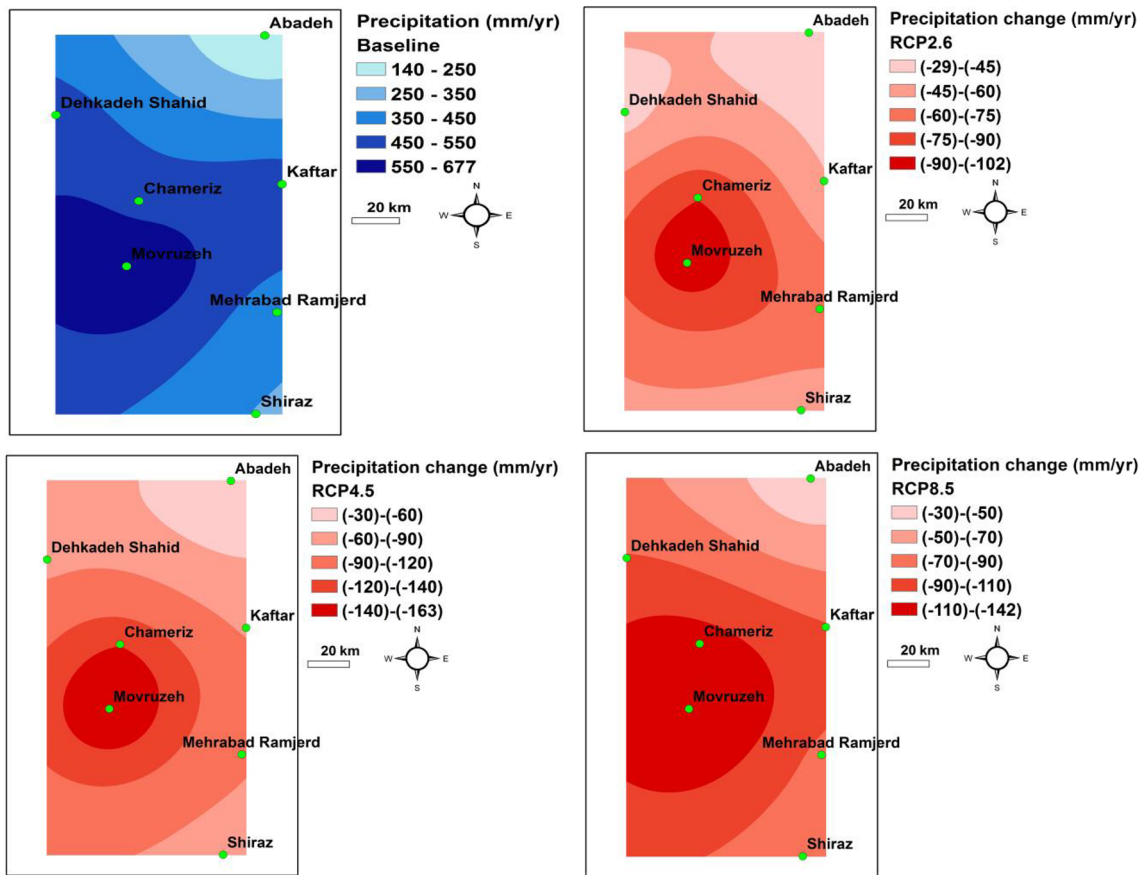


Fig. 6 The spatial distribution map of mean annual precipitation during the baseline period (1978–2005) and change in mean annual precipitation during the period 2026–2085 under three RCPs

of climate change on water resources. Therefore, in this study, 5-year time windows are selected to calculate change factors using each CMIP5 model, making outputs of this study applicable for water resource managers and planners. Transient change factors for each climatic station are calculated using daily output of the nearest grid center of a given CMIP5 model.

3.4 Standardized precipitation index analysis

Standardized precipitation index (SPI) developed by McKee et al. (1993) is used to determine droughts and wet periods in northern Fars Province for the present time and under three RCPs. The SPI is the most commonly used method for drought and wet year monitoring (Bonaccorso et al. 2003; Tsakiris and Vangelis 2004; Giorgi and Lionello 2008; Raziei et al. 2010, 2013; Javanmard et al. 2017) and a useful index to monitor wet and dry periods in regions with diverse hydrological regimes (Raziei et al. 2010). The SPI index is based on gamma cumulative distribution function (Almedejj 2014; Gumus and Algin 2017).

$$G(x) = \frac{1}{\beta \Gamma(\alpha)} \int_0^x t^{\alpha-1} e^{-\frac{t}{\beta}} dt \tag{1}$$

$$\Gamma(\alpha) = \int_0^\infty t^{\alpha-1} e^{-t} dt$$

where $G(x)$ is gamma cumulative distribution function, x measured precipitation, and $\Gamma(\alpha)$ gamma function. Coefficients α and β are shape and scale parameters, respectively, which can be calculated using the following equations (Almedejj 2014; Gumus and Algin 2017).

$$\alpha = \frac{1}{4A} \left(1 + \sqrt{1 + \frac{4A}{3}} \right) \tag{2}$$

$$A = \ln(\bar{x}) - \frac{\sum \ln(x)}{n}$$

$$\beta = \frac{\bar{x}}{\alpha}$$

in which n is number of measured precipitation and \bar{x} mean value of precipitation data.

Cumulative gamma distribution function $G(x)$ is defined for $x > 0$ (incomplete gamma distribution function) while

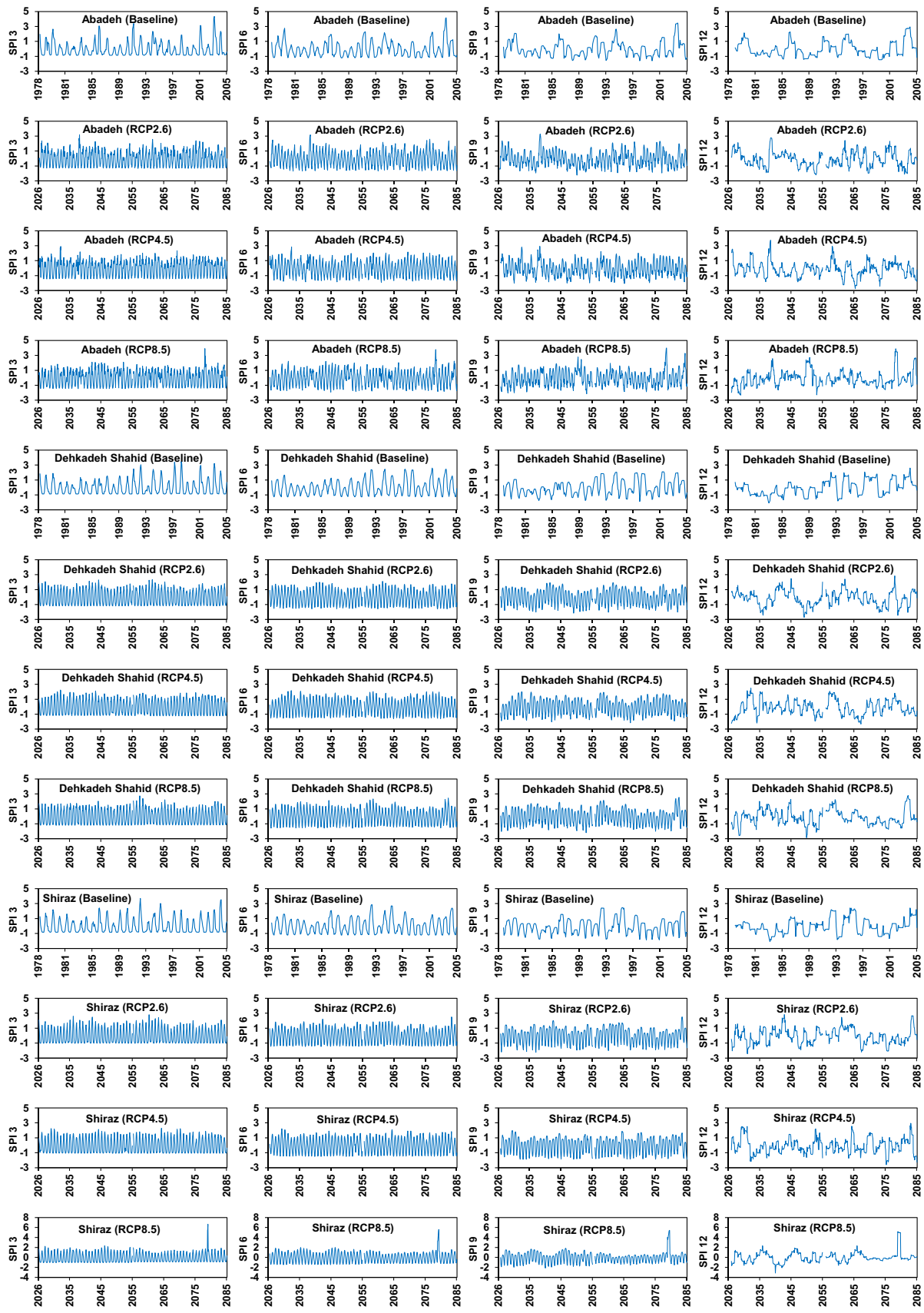


Fig. 7 The SPI time series (3-, 6-, 9-, and 12-month time scales) for three representative climatic stations (Abadeh, Dehkadeh Shahid, Shiraz) within the study area for the baseline period and three RCPs

precipitation measurement may contain zero values ($x = 0$). Complete cumulative gamma distribution function $H(x)$ is expressed as $H(x) = q + (1 - q)G(x)$ where q is the probability of no precipitation. The value of q is equal to the ratio of $\frac{m}{n}$ where m is the number of zero precipitation measurement throughout total number of n measurements (Almedeij 2014; Thom 1958).

Finally, gamma cumulative distribution function () is transformed into normal standardized distribution with a mean of zero and unit standard deviation using the following equations (Almedeij 2014).

$$SPI = -\left(t - \frac{c_0 + c_1t + c_2t^2}{1 + d_1t + d_2t^2 + d_3t^3}\right) \quad 0 < H(x) \leq 0.5 \tag{3}$$

$$SPI = +\left(t - \frac{c_0 + c_1t + c_2t^2}{1 + d_1t + d_2t^2 + d_3t^3}\right) \quad 0.5 < H(x) \leq 1 \tag{4}$$

where

$$t = \sqrt{\ln\left(\frac{1}{H(x)^2}\right)} \quad 0 < H(x) \leq 0.5$$

$$t = \sqrt{\ln\left(\frac{1}{1-H(x)^2}\right)} \quad 0.5 < H(x) \leq 1$$

Coefficients in Eqs. 3 and 4 are $c_0 = 2.515517$, $c_1 = 0.802853$, $c_2 = 0.010328$, $d_1 = 1.432788$, $d_2 = 0.189269$, and $d_3 = 0.001308$.

The SPI value greater than 1 indicates wet condition, value less than -1 indicates dry condition, and value between -1 and 1 implies a normal condition, see Table 4 (McKee et al. 1993). Wet, normal, and dry periods over the study area are monitored using 3-, 6-, 9-, and 12-month time scales of the SPI at baseline and future periods. A wet event begins with $SPI > 1$ and ends when $SPI < 1$ while a dry event begins with $SPI < -1$ and ends when $SPI > -1$. Duration of an event, for example for a dry event, is number of consecutive months that lie within that event (equal to end month minus first month). Severity of an event, for example, for a dry event, is absolute value of the integral area between the SPI line and horizontal axis ($SPI = 0$) (Almedeij 2014; Spinoni et al. 2014).

$$severity = \left| \sum_{i=1}^d SPI_i \right| \tag{5}$$

where i denotes number of month lie within an event (i starts with the first month of an event and continues until the end of that event) and d is the event duration.

Intensity for an event is defined as maximum absolute SPI value identified at that event (Almedeij 2014; Spinoni

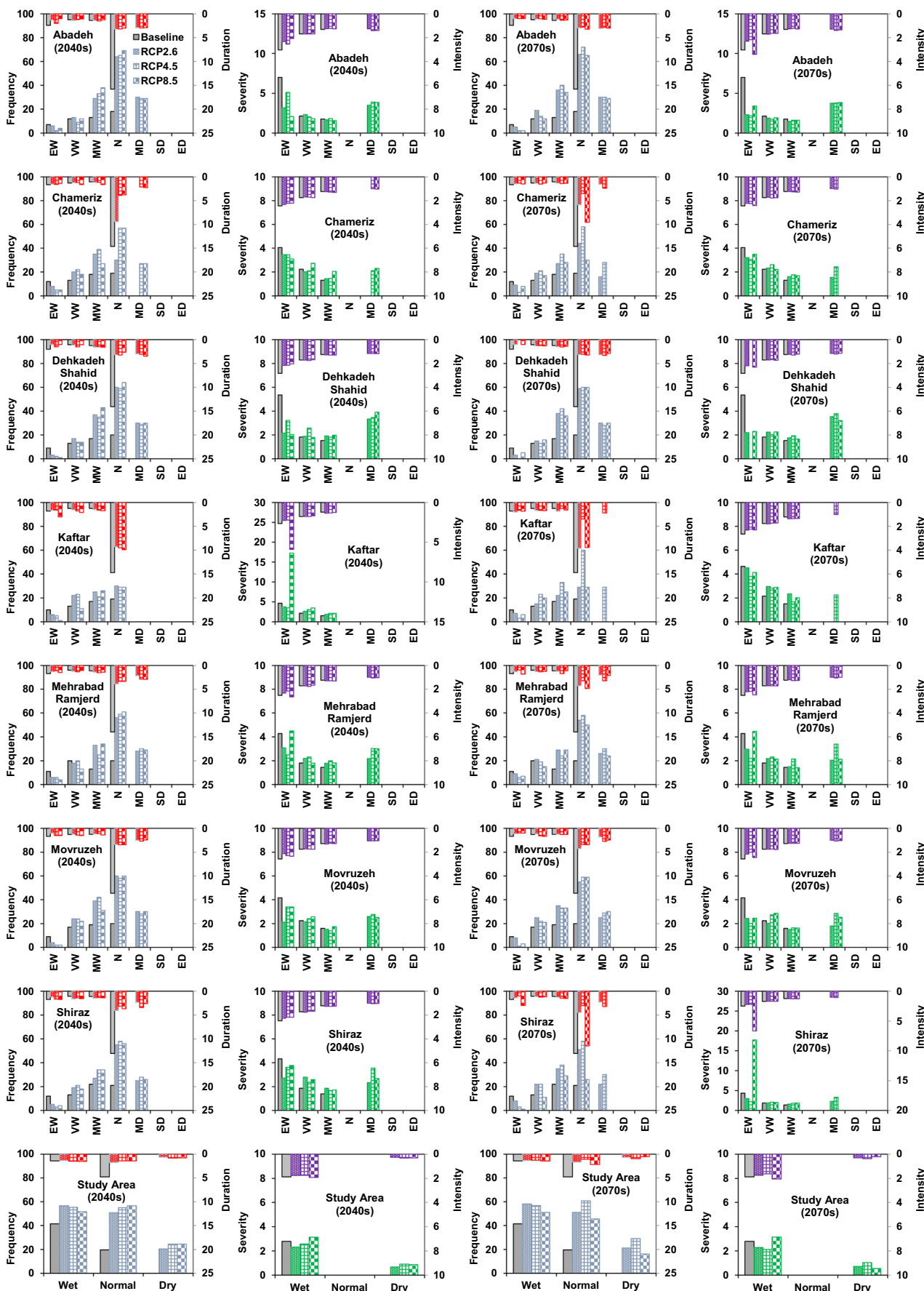
et al. 2014). Finally, frequency of specific events, for example drought frequency, is defined as number of drought events during the study period. It is worth to mention that all aforementioned parameters (frequency, duration, severity, intensity) are calculated for wet and dry periods at the baseline period and under three RCPs, but only frequency and duration parameters are calculated for normal periods because severity and intensity are not meaningful for normal periods.

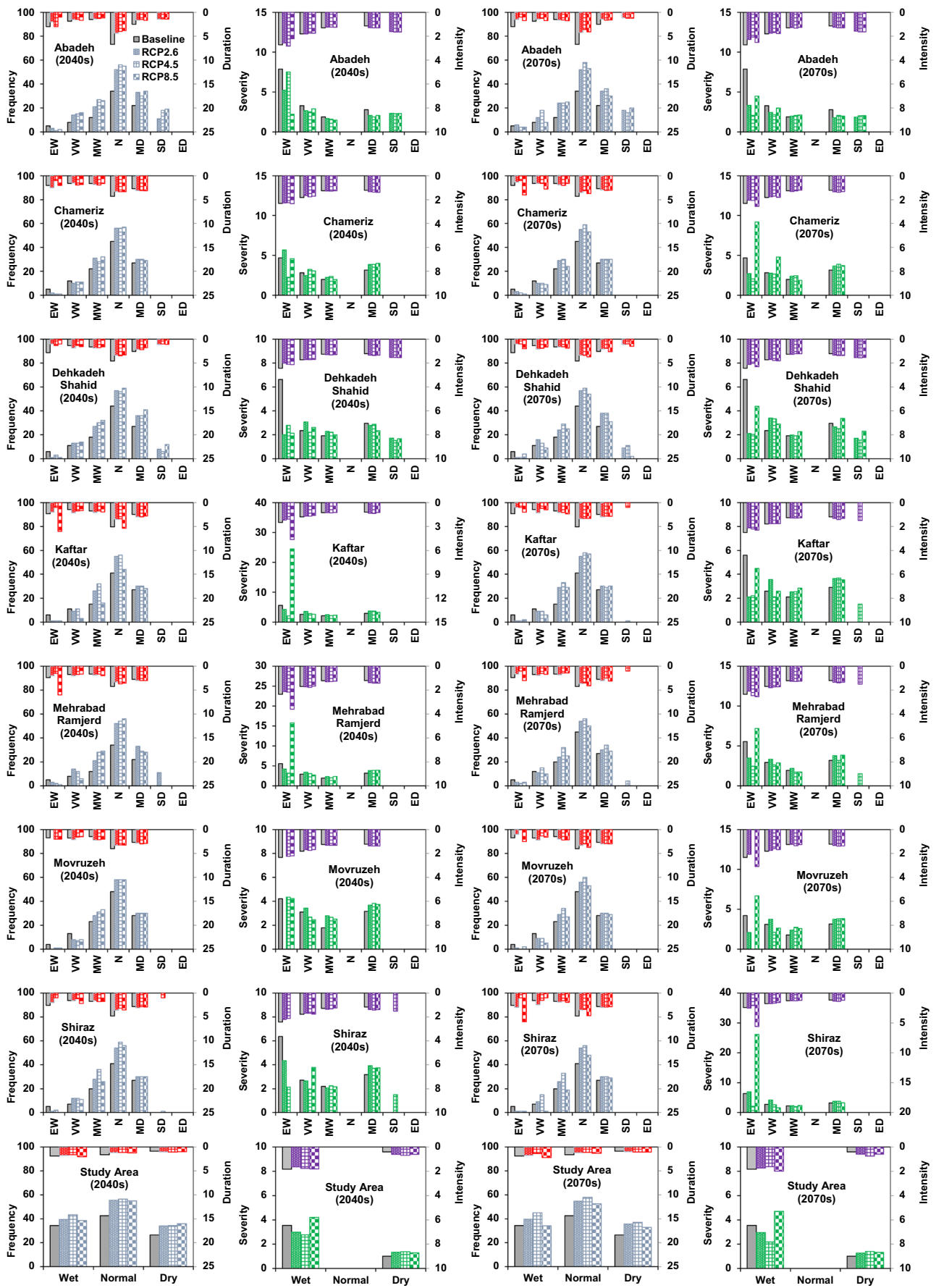
4 Results and discussion

4.1 Temperature and precipitation under climate change

Predicted annual temperature in Abadeh and Shiraz stations, based on CMIP5 ensemble, is presented for period 2026–2085 in Fig. 4. The annual temperature in Abadeh station is about 15.7°C in early twenty-first century under the three RCPs, but it will increase to 16.2 , 17.6 , and 19.8°C at late twenty-first century under the RCP2.6, RCP4.5, and RCP8.5, respectively. The annual temperature in Shiraz station is about 19.9°C in early twenty-first century under climate change, but it will increase to 20.3 , 21.7 and 23.9°C at late twenty-first century under the RCP2.6, RCP4.5, and RCP8.5, respectively. The predicted change in mean annual temperature (2026–2085 relative to the baseline period) for two stations using each GCM is presented in Fig. 4. The temperature anomaly for Abadeh station varies from $+1.1$ to $+2.3^\circ\text{C}$ in RCP2.6, $+1.8$ to $+3.3^\circ\text{C}$ in RCP4.5 and $+1.8$ to $+4.2^\circ\text{C}$ in RCP8.5. The temperature anomaly for Shiraz station varies from $+1.2$ to $+2.4^\circ\text{C}$ in RCP2.6, $+1.8$ to $+3.4^\circ\text{C}$ in RCP4.5 and $+1.9$ to $+4.4^\circ\text{C}$ in RCP8.5. Downscaled temperature based on the CMIP5 ensemble shows that mean annual temperature in Abadeh station will increase from 14.3°C during the baseline period (1978–2005) to 16.1 , 16.7 , and 17.7°C under the RCP2.6, RCP4.5, and RCP8.5, respectively, leading to an increase by $+1.8$, $+2.4$, and $+3.4^\circ\text{C}$, respectively (Fig. 4). The mean annual temperature in Shiraz station will increase from 18.3°C during the baseline period to 20.2 , 20.85 , and 21.8°C under the RCP2.6, RCP4.5, and RCP8.5, respectively, leading to an increase by $+1.9$, $+2.55$, and $+3.5^\circ\text{C}$, respectively (Fig. 4). Therefore, it may be concluded, based on the average temperature anomaly of these stations, that the

Fig. 8 The 3-month SPI analysis for seven climatic stations and study area during the baseline period (1978–2005) and future periods 2026–2055 (2040s) and 2056–2085 (2070s) under the three RCPs. EW, extremely wet; VW, very wet; MW, moderately wet; N, near normal; MD, moderately dry; SD, severely dry; ED, extremely dry. Blue, red, green, and violet bars show frequency, duration, severity, and intensity values, respectively





◀ **Fig. 9** The 6-month SPI analysis for seven climatic stations and study area during the baseline period (1978–2005) and future periods 2026–2055 (2040s) and 2056–2085 (2070s) under the three RCPs. EW, extremely wet; VW, very wet; MW, moderately wet; N, near normal; MD, moderately dry; SD, severely dry; ED, extremely dry. Blue, red, green, and violet bars show frequency, duration, severity, and intensity values, respectively

mean annual temperature over the study area will increase by about 1.85, 2.5, and 3.45 °C under the RCP2.6, RCP4.5, and RCP8.5, respectively.

Daily precipitation data of each CMIP5 model is transiently downscaled to seven climatic stations under the three RCPs. The predicted percentage change in mean annual precipitation of each climatic station for the period 2026–2085 is compared with that value of period 1978–2005 (Fig. 5). The percentage change of precipitation differs among the stations, RCPs, and GCMs. The precipitation anomaly at each station and specific RCP varies from positive to negative values among the different GCMs, but dominant precipitation anomaly is negative. The ranges of precipitation anomaly in stations of Abadeh, Chameriz, Dehkadeh Shahid, Kaftar, Mehrabad Ramjerd, Movruzeh, and Shiraz are +7.9 to –46.6%, +23.1 to –49.1%, +28.6 to –29.2%, +47.8 to –30.1%, +27.1 to –47.4%, +21.9 to –43.7%, and +20.5 to –40% under the RCP2.6, respectively; –4.3 to –48.6%, +13.3 to –68.2%, +17 to –53.5%, +28 to –61.4%, +27 to –61.7%, –0.7 to –67%, and +11 to –58% under the RCP4.5; and +12.1 to –47.9%, +55.5 to –62.4%, +39 to –45%, +43.1 to –50.4%, +42.2 to –55%, +31.5 to –57%, and +30.6 to –54.6% under the RCP8.5, respectively. Downscaled precipitation based on the CMIP5 ensemble reveals that stations of Abadeh, Chameriz, Dehkadeh Shahid, Kaftar, Mehrabad Ramjerd, Movruzeh, and Shiraz will experience a precipitation reduction of 20.7, 18.2, 7.4, 8.9, 17.8, 14.7, and 15.6% under the RCP2.6, a precipitation reduction of 22.1, 28.3, 16, 16.9, 25, 24.2, and 22% under the RCP4.5 and finally a precipitation reduction of 21.8, 23.7, 18, 17.9, 22.4, 31.3, and 21.7% under the RCP8.5, respectively (Fig. 5). Therefore, the study area will experience a precipitation reduction under climate change. The mean annual precipitation over the study area is 437 mm during the period 1978–2005 (Fig. 6), but it will reduce to 376, 341, and 346 mm in the RCP2.6, RCP4.5, and RCP8.5, respectively, leading to the percentage reductions of 14, 22, and 20.8%, respectively. The mean annual precipitation changes under three RCPs during the period 2026–2085 relative to baseline period (1978–2005) are presented in Fig. 6. The study area will experience a precipitation reduction of 29–102, 30–163, and 30–142 mm/year under the RCP2.6, RCP4.5, and RCP8.5, respectively. The spatial distribution of precipitation reduction indicates that the southwestern regions having higher precipitation will experience greater

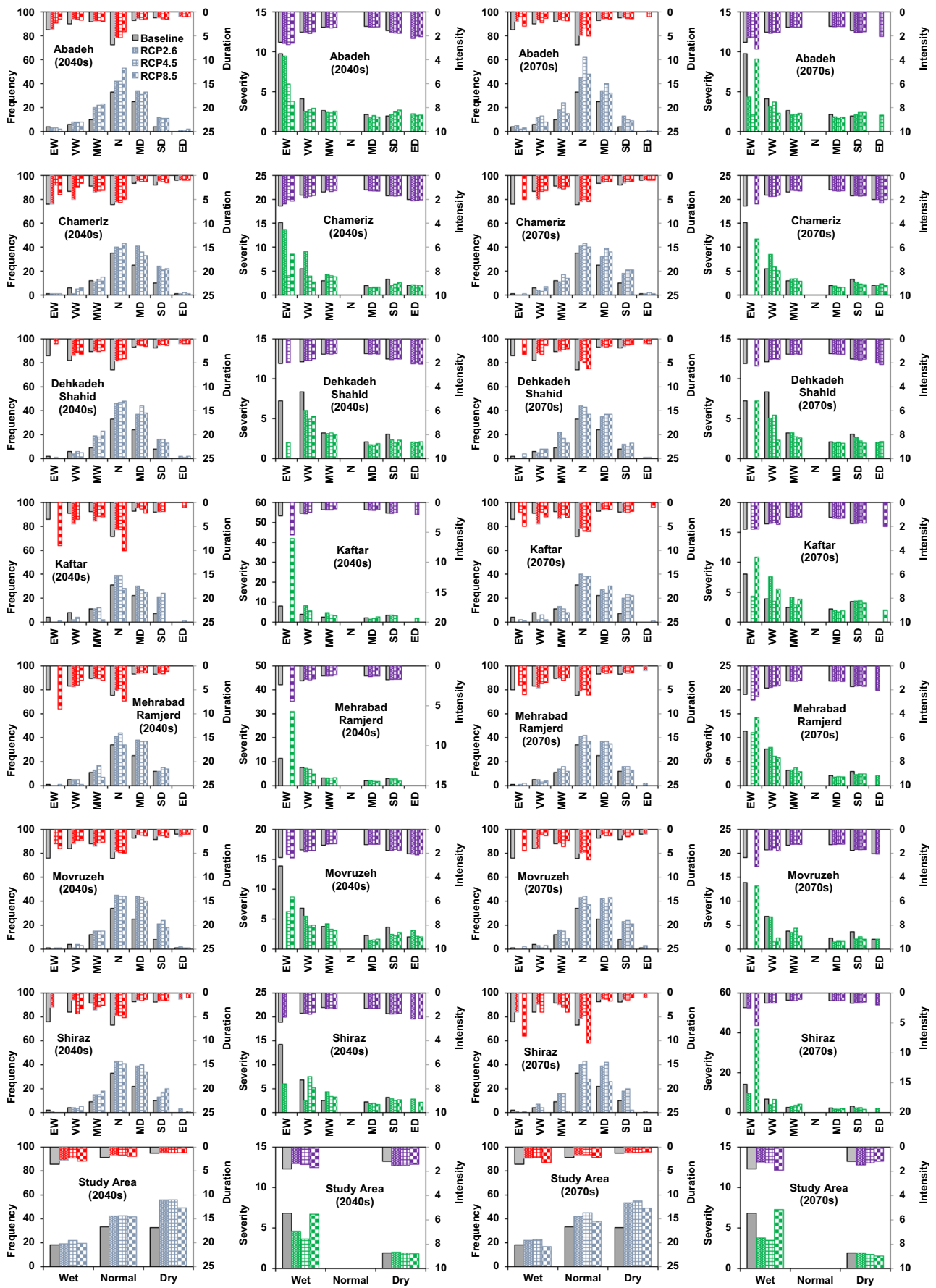
precipitation reduction in the future. Precipitation originates from three sources of the Mediterranean Sea, Red Sea, and Indian Ocean monsoons that contributes to annual precipitation of the study area by 74, 23, and 3%, respectively (Alijani and Harman 1985; Beyglou et al. 2009; Parab Consulting Engineers 1996; Roshani et al. 2013). Climate change studies by Ulbrich et al. (2006), Mariotti et al. (2008), Giorgi and Lionello (2008), Evans (2008), and Evans and Alsamawi (2011) indicate that the contribution of the Mediterranean air masses will reduce due to the reduction of cyclogenesis while contributions of southern water bodies such as the Red Sea and Persian Gulf will increase under global warming. Climate change in the study area is substantially influenced by the Mediterranean Sea and, in second order of importance, by Red Sea based on their annual contributions in precipitation events. Therefore, resultant of climate change in moisture sources of the Mediterranean and Red Seas will lead to precipitation reduction in northern Fars Province.

4.2 Drought and wet years under climate change

Water resources are sensitive to duration of wet years and droughts especially in arid and semi-arid regions where water demand is mainly supplied by surface water and groundwater due to the limited precipitation (Meigh et al. 2002; Shatanawi et al. 2013). The prolonged droughts associated with increase of water demand under climate change will lead to further water shortage in a given region.

Downscaled daily precipitation data based on the ensemble of CMIP5 models is used to determine wet year and droughts at each station. Droughts and wet and normal periods for each climatic station are determined using 3-, 6-, 9-, and 12-month timescales of the SPI method. The wet, normal, and dry periods are calculated for 28-year baseline period (1978–2005) and future 30-year periods 2026–2055 (2040s) and 2056–2085 (2070s), under the three RCPs. The SPI time series (3-, 6-, 9-, and 12-month time scales) for three representative stations (Abadeh, Dehkadeh Shahid, Shiraz) for the baseline period and three climate change scenarios are presented in Fig. 7.

The 3-month SPI analysis indicate that wet periods are dominant over the study area while no drought has occurred during the baseline period (Fig. 8). Frequency of wet, normal, and dry periods will increase during the period 2040s under the three RCPs. Duration of wet years will not change significantly during this period, but duration of normal periods will decrease. As droughts will occur in the future, duration of dry periods will increase in the period 2040s. Severity and intensity of wet periods will not change significantly, however, severity and intensity of droughts will increase under the three RCPs. Results are the same for second period 2070s (Fig. 8). Overall, 3-month SPI analysis reveals that frequency of wet years will increase under climate change while duration,



◀ **Fig. 10** The 9-month SPI analysis for seven climatic stations and study area during the baseline period (1978–2005) and future periods 2026–2055 (2040s) and 2056–2085 (2070s) under the three RCPs. EW, extremely wet; VW, very wet; MW, moderately wet; N, near normal; MD, moderately dry; SD, severely dry; ED, extremely dry. Blue, red, green, and violet bars show frequency, duration, severity, and intensity values, respectively

severity, and intensity will not change significantly. All frequency, duration, severity, and intensity of droughts will increase in the future due to climate change.

The 6-month SPI analysis indicate that frequency of wet, normal, and dry periods will increase during both periods 2040s and 2070s under the three RCPs (Fig. 9). Duration of wet and dry periods will not change significantly, but duration of normal periods will slightly decrease from 1.6 months at baseline period to about 1.2 months under three RCPs. Severity of wet periods will decrease (except in RCP8.5) while severity of droughts will increase under global warming (Fig. 9). Intensity of wet periods will not change under climate change; however, droughts will be intensified. The 6-month SPI analysis, in summary, shows that frequency of wet periods will increase but severity will decrease; however, duration and intensity will not change under three RCPs. Drought duration will not change considerably in the future; however, the study area will experience more frequent, severed, intensified droughts due to climate change.

The 9-month SPI analysis indicate that frequency of wet periods will not change during both periods 2040s and 2070s under the three RCPs, but frequencies of normal and dry periods will increase in the future (Fig. 10). Duration of wet and normal periods will decrease, but duration of droughts will not change significantly under three RCPs. Severity of wet periods will decrease (except in RCP8.5) while severity of droughts will not change noticeably under global warming (Fig. 10). Intensity of wet periods will decrease under climate change; however, droughts will slightly be intensified. Overall, frequency of wet periods will not change, but all duration, severity, and intensity will decrease under climate change. The study area will experience more frequent, intensified droughts in the future due to global warming.

The 12-month SPI represents well the annual precipitation patterns (Bonaccorso et al. 2003; Tsakiris and Vangelis 2004). The 12-month SPI analysis indicate that frequency of wet and normal periods over the study area will decrease during both periods 2040s and 2070s under three RCPs but drought frequency will slightly increase, except in RCP8.5 (Fig. 11). For example, frequency of wet, normal, and dry periods is 20, 21, and 18 during the baseline period, respectively, while frequency of these periods is 15, 17, and 20 during the period 2070s under RCP4.5. Duration of wet, normal, and dry periods will increase under climate change, except for decreased drought duration under the RCP8.5. For example, duration of wet,

normal, and dry periods is 2.7, 3.3, and 2.8 months during the baseline period, respectively, while duration of these periods is 3, 5.8, and 3.8 months during the period 2040s under the RCP4.5 (Fig. 11). Results show that severity of wet and dry periods will increase under climate change. Intensity of wet periods will not change significantly; however, droughts will slightly be intensified under climate change. The 12-month SPI analysis, in summary, indicates that frequency of wet periods will decrease, duration and severity will increase while intensity will not change expressively under global warming. Frequency, duration, severity, and intensity of droughts will increase under climate change; therefore, the study area will experience more frequent, longer-duration, severed, intensified droughts under global warming.

Monitoring wet, normal, and dry periods using SPI analysis during the baseline period and under three RCPs reveal that detection of change in frequency, duration, severity, and intensity of each extreme climate event depends on the time scale of the SPI (Table 5). For example, 3-month SPI analysis shows that frequency of wet periods will increase under climate change, but other parameters (duration, severity, and intensity) will not change significantly. The 12-month SPI analysis indicate that frequency of wet periods will decrease but duration and severity will increase due to global warming. Results for normal periods are more consistent in which most SPI time scales (3, 6, and 9 months) result in increased frequency and decreased duration; however, 12-month SPI analysis shows decreased frequency and increased duration. Most SPI time scales result in more frequent, longer-duration, severed, intensified droughts under climate change for northern Fars Province in southern Iran.

4.3 Extreme storms under climate change

Extreme storm in a given year is defined as maximum daily precipitation that occurs (Chow et al. 1988). The annual maximum series at each climatic station for the baseline period (1978–2005) and future 30-year periods 2026–2055 (2040s) and 2056–2085 (2070s) are developed using time series of maximum daily precipitations (Chow et al. 1988). The annual maximum series under the three RCPs are developed based on the mean of multi-model downscaling results. The Kolmogorov–Smirnov and Chi-squared tests are used at a significance level of 0.05 to find the best fitted statistical distributions on annual maximum series. Goodness of fit on statistical distributions of exponential (1P and 2P), gamma (2P and 3P), general gamma (3P and 4P), log-gamma (2P), general extreme value, normal, log-normal (2P and 3P), Pearson (2P and 3P), and log-Pearson (3) shows that the general extreme value is best-fitted statistical distribution. The density function of the general extreme value distribution is defined by three parameters of scale, shape, and location (Chow et al. 1988). These three parameters are estimated at each climatic

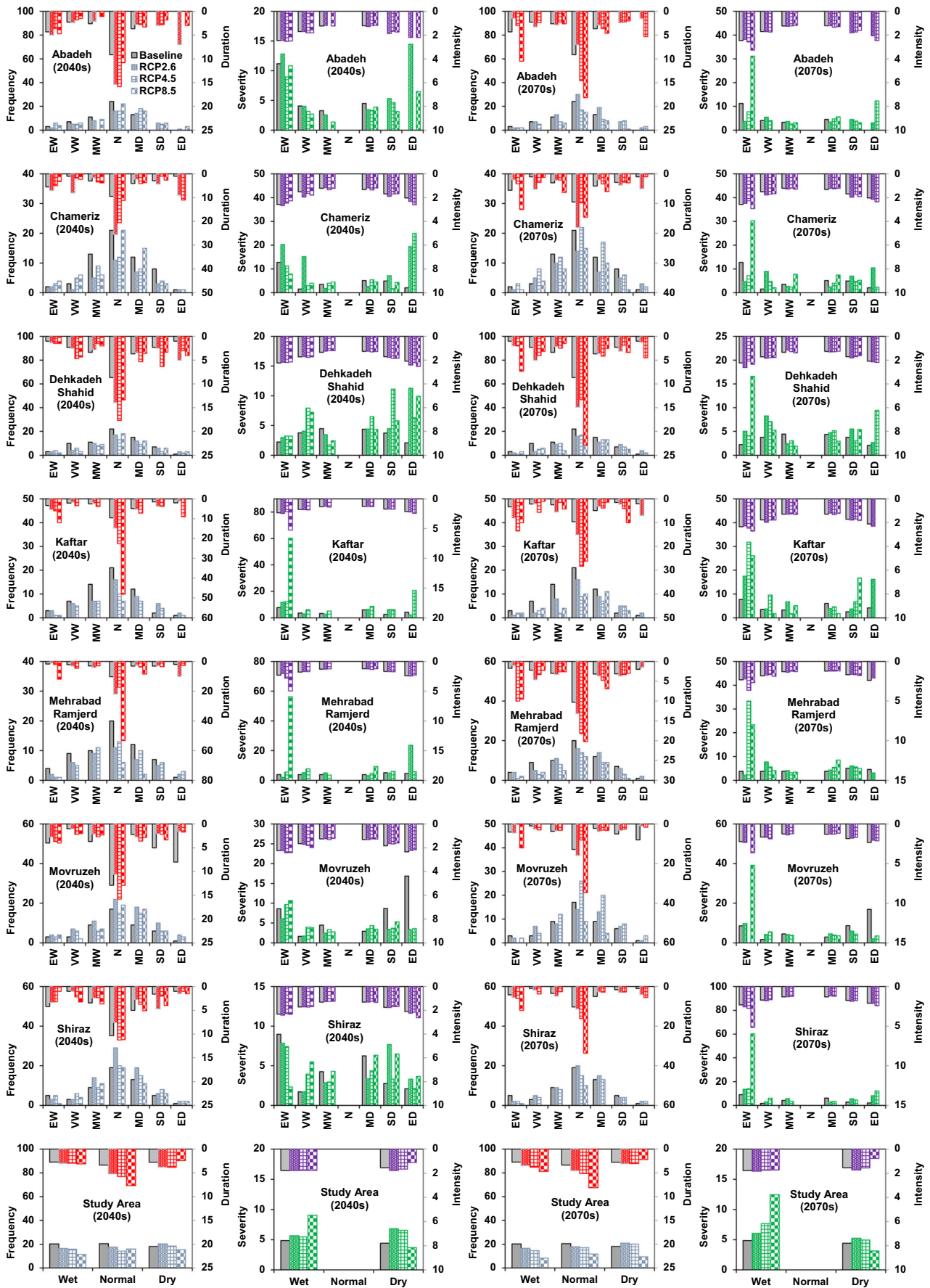


Fig. 11 The 12-month SPI analysis for seven climatic stations and study area during the baseline period (1978–2005) and future periods 2026–2055 (2040s) and 2056–2085 (2070s) under the three RCPs. EW, extremely wet; VW, very wet; MW, moderately wet; N, near normal; MD, moderately dry; SD, severely dry; ED, extremely dry. Blue, red, green, and violet bars show frequency, duration, severity, and intensity values, respectively

station for the baseline period and future periods 2040s and 2070s. Then, precipitation depths of extreme storms for different return periods (2, 5, 10 and 20 years) are determined using the fitted general extreme value distribution function (Fig. 12).

The precipitation depth of 2-year return period storms will increase from 51 mm at the baseline period (1978–2005) to about 61 mm under the three RCPs and two future periods (Fig. 12). The precipitation depth of 5-year return period storms (69.5 mm) will significantly not change under the three RCPs and two future periods due to the predicted minimum and maximum values of 67 and 73 mm, respectively. But the precipitation depth of 10- and 20-year return period storms will decrease under the three RCPs and two periods. The precipitation depth of 10-year return period storms (83 mm) will reduce to 80, 71, and 77 mm at period 2040s, and 72.5, 73, and 81 mm at period 2070s under the RCP2.6, RCP4.5, and RCP8.5, respectively. The precipitation depth of 20-year return period storms (96 mm) will decrease to 85.5, 76, and 85 mm at period 2040s and 76, 80, and 91 mm at period 2070s under the RCP2.6, RCP4.5, and RCP8.5, respectively. The extreme storms’ analysis under climate change shows that the precipitation depth of 2-year return period storms will increase, precipitation depth of 5-year return period storms will not change, but precipitation depth of 10- and 20-year return period storms will decrease under global warming.

In this study, precipitation depth of extreme storms having different return periods are determined using downscaled daily precipitation data for the baseline period and three RCPs. As mentioned before, precipitation depth of an extreme storm is defined as “maximum depth of daily precipitation that occurs during a given year.” It is worth mentioning that this concept differs to “storm intensity” which is defined as

“precipitation depth falls during the storm period (precipitation depth/storm period).” The latter is determined using hourly data and expressed, for example, as millimeters per hour. Therefore, as extreme storm analysis indicates that precipitation depth of 10- and 20-year return period storms will decrease under climate change, storm intensity may decrease, increase, or not change under global warming, and it requires further analysis using hourly precipitation data under climate change.

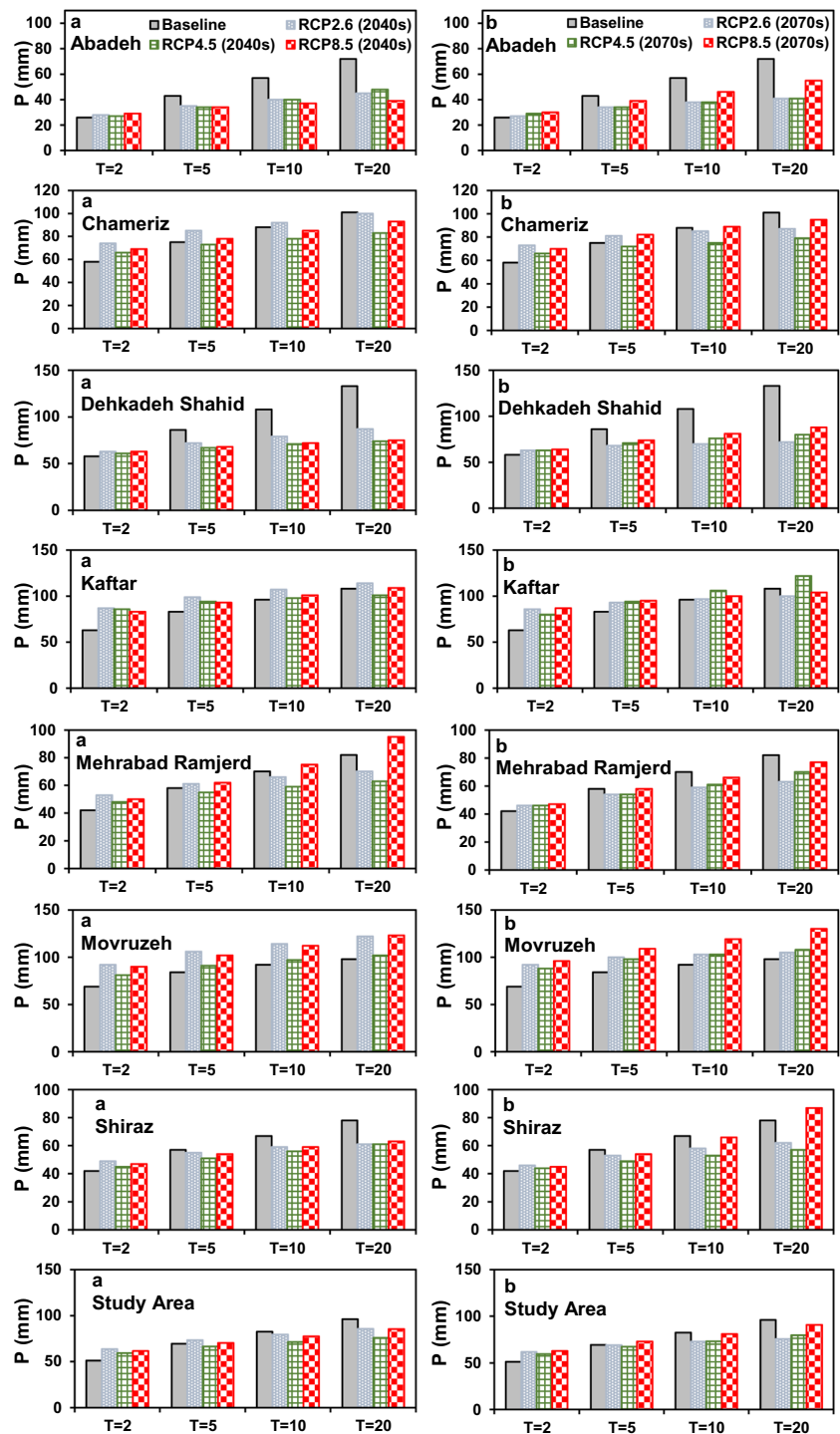
Climate change studies in Iran (see Table 1) indicate that detection of the future change in precipitation and temperature depends on the geographical location, global warming scenarios, number of used GCMs, and period of the study. Downscaling results in this study show that the mean annual precipitation in northern Fars Province will decrease (14–22%) under three RCPs. Babaeian et al. (2015) dynamically downscaled output of one GCM (HadAM3p) over the study area for the future period 2071–2100. They found that precipitation will decrease by 30 and 35% under scenarios B2 and A2, respectively. Later, Karandish et al. (2017) statistically downscaled outputs of 15 GCMs over Iran under scenarios B1, A1B, and A2 in which only one climatic station (Abadeh) was used over the study area. Precipitation in Abadeh is predicted to increase by 10% in the future. Vaghefi et al. (2019) statistically downscaled outputs of five GCMs in Iran under RCP4.5 and RCP8.5 while no climatic station was selected over the study area. They found that precipitation will decrease by 25 mm in the future using interpolated surrounding precipitation anomalies. Overall, most climate change studies reveal a precipitation reduction over the study area; however, the percentage change varies due to difference in period of study, number of used GCMs, number of climatic stations, and selected scenarios.

In this study, mean annual temperature is predicted to increase by 1.85–3.45 °C over the study area under three RCPs. Climate change studies by Babaeian et al. (2015) and Karandish et al. (2017) showed that the study area will warm by about 1–5 °C under three scenarios B1, A1B, and A2. However, new scenarios which are used in this study (RCPs) differ from those in previous studies, but the predicted

Table 5 Summary of change in frequency, duration, severity, and intensity of extreme climate events using 3-, 6-, 9-, and 12-month timescales of SPI under global warming

SPI	Wet period				Normal period		Dry period			
	Frequency	Duration	Severity	Intensity	Frequency	Duration	Frequency	Duration	Severity	Intensity
3	Increase	No change	No change	No change	Increase	Decrease	Increase	Increase	Increase	Increase
6	Increase	No change	Decrease	No change	Increase	Decrease	Increase	No change	Increase	Increase
9	No change	Decrease	Decrease	Decrease	Increase	Decrease	Increase	No change	No change	Increase
12	Decrease	Increase	Increase	No change	Decrease	Increase	Increase	Increase	Increase	Increase

Fig. 12 The precipitation depth (P) of extreme storms having different return periods (T) for the baseline period (1978–2005) and future periods 2026–2055 (2040s) and 2056–2085 (2070s) under the three RCPs



range of temperature increase (1.85–3.45 °C) is within that range provided by previous studies (1–5 °C).

Results show that frequency, duration, severity, and intensity of droughts and precipitation depth of most-frequent storms (2-year return period storms) will increase over the study area while precipitation depth of less-frequent storms (10- and 20-year return period storms) will reduce due to climate change. Results of the previous studies across the

country and study area, based on the observed precipitation and temperature data at climatic stations, are as follows:

i. The long-term observed precipitation and temperature data at climatic stations in Iran indicates that annual temperature has increased by 0.2 °C and annual precipitation has decreased by 8 mm/decade, frequency of light precipitation (< 10 mm) have increased while frequency of heavy (25–50 mm) and extremely heavy (> 50 mm) precipitations have decreased

(Alizadeh-Choobari and Najafi 2018; Ghiami-Shamami et al. 2019; Modarres et al. 2016; Soltani et al. 2016). Generally, studies show that frequency, intensity, and duration of droughts will also increase under climate change in different regions of the country, especially in arid and semi-arid regions (Ahmadebrahimpour et al. 2019; Dastorani et al. 2011; Fadia Maghsood et al. 2019; Modarres et al. 2018; Roshan et al. 2013; Vaghefi et al. 2019).

ii. Climate studies over the study area shows that duration and severity of droughts have increased during long-term observation period 1950–2010 due to observed warming during this period (Modarres et al. 2016). Precipitation depth of heavy and extremely heavy events have significantly reduced over the study area during the observation period 1975–2010 while the number of consecutive dry days have increased (Soltani et al. 2016).

Results of this study, which predict more frequent, longer-duration, severed, intensified droughts and increased precipitation depth of frequent storms (2-year return period storms), seem to be reliable as there is a consistency between projected results with observed anomalies over the study area.

5 Conclusion

Daily precipitation and minimum and maximum temperature data generated by 22 CMIP5 models are transiently down-scaled to seven climatic stations using the LARS-WG over northern Fars Province in southern Iran, under the RCP2.6, RCP4.5, and RCP8.5. Results show that the study area will warm by +1.85, +2.5, and +3.45 °C under the RCP2.6, RCP4.5, and RCP8.5, respectively, while precipitation will reduce by 14, 22, and 20.8%, respectively. Precipitation is mainly affected by the Mediterranean air masses and, in second order, by Red Sea air masses (Alijani and Harman 1985; Beyglou et al. 2009; Parab Consulting Engineers 1996; Roshani et al. 2013). Climate change studies show that precipitation source of the Mediterranean Sea will reduce but water vapor fluxes from the Red Sea will increase (Evans 2008; Evans and Alsamawi 2011; Evans 2009; Giorgi and Lionello 2008; Mariotti et al. 2008; Ulbrich et al. 2006). Therefore, resultant of climate change in the moisture sources of the Mediterranean Sea and Red Sea will lead to the precipitation reduction over the study area due to high contribution of the Mediterranean air masses (74%).

Monitoring wet, normal, and dry periods using SPI analysis during the baseline period and under three RCPs reveals that detection of change in frequency, duration, severity, and intensity of each extreme climate event depends on time scale of the SPI. Analysis, in summary, shows that frequency (duration) of normal periods will increase (decrease) under climate change; however, 12-month SPI analysis shows decreased frequency and increased duration for normal periods.

Frequency, duration, severity, and intensity of wet periods may increase, decrease, or not change under climate change, depending on the SPI time scale. The study area will experience more frequent, longer-duration, severed, intensified droughts in the future due to global warming. Results for shorter time scale of the SPI may not be representative of extreme climate events due to avoiding dry months while longer time scales of the SPI seem to be more representative of extreme climate events because larger months are incorporated for analysis.

Extreme storm analysis under climate change shows that precipitation depth of 2-year return period storms will increase, precipitation depth of 5-year return period storms will not change, but precipitation depths of 10- and 20-year return period storms will decrease under global warming. The surface and subsurface water resources of the study area are continually depleted, especially in recent years, due to recent intense droughts and water over-exploitation. The raised temperature will increase potential evapotranspiration which, in turn, increases crops' water demand, especially in arid regions. Precipitation reduction associated with more frequent, prolonged, severed, intensified droughts will lead to more water shortage within the study area. Knowledge of extreme climate events under climate change in northern Fars Province is useful and vital for sustainable water resource management and planning in the future.

Acknowledgments Help of the Iranian Water Resources Management Company and Iranian Meteorological Organization in providing the weather data is greatly appreciated.

Funding The author is thankful for support from the Institute for Advanced Studies in Basic Sciences of Zanjan, Iran.

References

- Aguilera H, Murillo J (2009) The effect of possible climate change on natural groundwater recharge based on a simple model: a study of four karstic aquifers in SE Spain. *Environ Geol* 57:963–974
- Ahmadebrahimpour E, Aminnejad B, Khalili K (2019) Assessing future drought conditions under a changing climate: a case study of the Lake Urmia Basin in Iran. *Water Supply*
- Alijani B, Harman JR (1985) Synoptic climatology of precipitation in Iran. *Annals of the Association of American Geographers* 75:404–416. <https://doi.org/10.1111/j.1467-8306.1985.tb00075.x>
- Ali R, McFarlane D, Varma S, Dawes W, Emelyanova I, Hodgson G (2012) Potential climate change impacts on the water balance of regional unconfined aquifer systems in South-Western Australia. *Hydrol Earth Syst Sci* 16:4581–4601
- Alizadeh-Choobari O, Najafi M (2018) Extreme weather events in Iran under a changing climate. *Climate Dynamics* 50:249–260
- Almedej J (2014) Drought analysis for Kuwait using standardized precipitation index. *The Scientific World Journal*:2014
- Babaecian I, Modirian R, Karimian M, Zarghami M (2015) Simulation of climate change in Iran during 2071–2100 using PRECIS regional climate modelling system. *Desert* 20:123–134

- Bannayan M, Rezaei EE (2014) Future production of rainfed wheat in Iran (Khorasan province): climate change scenario analysis. *Mitigation and Adaptation Strategies for Global Change* 19:211–227
- Berg N, Hall A (2015) Increased interannual precipitation extremes over California under climate change. *Journal of Climate* 28:6324–6334
- Beyglou M, Khoshakhlagh F, Ovi R (2009) The seasonal location and frequency of cyclone tracks of wet periods in middle-western Iran. *Natl Geogr Res* 68:71–84. <https://doi.org/10.1007/s11069-015-1862-z>
- Bonaccorso B, Bordini I, Cancelliere A, Rossi G, Sutera A (2003) Spatial variability of drought: an analysis of the SPI in Sicily. *Water Resour Manag* 17:273–296
- Candela L, von Igel W, Elorza FJ, Aronica G (2009) Impact assessment of combined climate and management scenarios on groundwater resources and associated wetland (Majorca, Spain). *J Hydrol* 376: 510–527
- Chow V, Maidment D, Mays L (1988) *Applied hydrology* Editions McGraw-Hill, New York, 572 pp
- Dai A (2011) Drought under global warming: a review. *Wiley Interdiscip Rev Clim Chang* 2:45–65
- Dastorani M, Bavani A, Poormohammadi S, Rahimian M (2011) Assessment of potential climate change impacts on drought indicators (case study: Yazd station, Central Iran). *Desert* (2008-0875) 16
- De Martonne E (1926) *Aréisme et indice d'aridité*. Gauthier-Villars
- Etemadi H, Samadi SZ, Sharifikia M, Smoak JM (2016) Assessment of climate change downscaling and non-stationarity on the spatial pattern of a mangrove ecosystem in an arid coastal region of southern Iran. *Theoretical and Applied Climatology* 126:35–49
- Evans J (2008) Changes in water vapor transport and the production of precipitation in the eastern fertile crescent as a result of global warming. *J Hydrometeorol* 9:1390–1401
- Evans JP (2009) 21st century climate change in the Middle East. *Clim Chang* 92:417–432
- Evans JP (2010) Global warming impact on the dominant precipitation processes in the Middle East. *Theoretical and Applied Climatology* 99:389
- Evans J, Alsamawi A (2011) The importance of the Zagros Mountains barrier jet to future precipitation in the Fertile Crescent. *Open Atmospheric Science Journal* 5:87–95
- Fadia Maghsood F, Moradi H, Bavani M, Reza A, Panahi M, Berndtsson R, Hashemi H (2019) Climate change impact on flood frequency and source area in northern Iran under CMIP5. *Scenarios Water* 11: 273
- Fakhri M, Farzaneh MR, Eslamian S, Khordadi MJ (2012) Confidence interval assessment to estimate dry and wet spells under climate change in Shahrekord Station. *Iran Journal of Hydrologic Engineering* 18:911–918
- Fars Agriculture Organization (2017) *Statistical report on agriculture in Fars Province [In Persian]*
- Ghiami-Shamami F, Sabziparvar AA, Shinoda S (2019) Long-term comparison of the climate extremes variability in different climate types located in coastal and inland regions of Iran. *Theoretical and Applied Climatology* 136:875–897
- Giorgi F, Lionello P (2008) Climate change projections for the Mediterranean region. *Global and Planetary Change* 63:90–104
- Gohari A, Eslamian S, Abedi-Koupaei J, Bavani AM, Wang D, Madani K (2013) Climate change impacts on crop production in Iran's Zayandeh-Rud River Basin. *Science of the Total Environment* 442:405–419
- Green TR et al (2011) Beneath the surface of global change: impacts of climate change on groundwater. *J Hydrol* 405:532–560. <https://doi.org/10.1016/j.jhydrol.2011.05.002>
- Gumus V, Algin HM (2017) Meteorological and hydrological drought analysis of the Seyhan–Ceyhan River basins. *Turkey Meteorological Applications* 24:62–73
- Ho JT, Thompson JR, Brierley C (2016) Projections of hydrology in the Tocantins-Araguaia Basin, Brazil: uncertainty assessment using the CMIP5 ensemble. *Hydrol Sci J* 61:551–567
- Iizumi T, Semenov MA, Nishimori M, Ishigooka Y, Kuwagata T (2012) ELPIS-JP: a dataset of local-scale daily climate change scenarios for Japan. *Phil Trans R Soc A* 370:1121–1139
- Javanmard S, Emamhadi M, BodaghJamali J, Didehvarasl A (2017) Spatial–temporal analysis of drought in Iran using SPI during a long-term period. *Earth Sci* 6:15
- Jiang R, Xie J, He H, Luo J, Zhu J (2015) Use of four drought indices for evaluating drought characteristics under climate change in Shaanxi, China: 1951–2012. *Nat Hazards* 75:2885–2903
- Kabiri R, Bai VR, Chan A (2015) Assessment of hydrologic impacts of climate change on the runoff trend in Klang watershed. *Malaysia Environ Earth Sci* 73:27–37
- Karandish F, Mousavi SS, Tabari H (2017) Climate change impact on precipitation and cardinal temperatures in different climatic zones in Iran: analyzing the probable effects on cereal water-use efficiency. *Stochastic Environmental Research and Risk Assessment* 31:2121–2146
- Knutti R, Sedláček J (2013) Robustness and uncertainties in the new CMIP5 climate model projections. *Nature Climate Change* 3:369
- Kousari MR, Zarch MA (2011) Minimum, maximum, and mean annual temperatures, relative humidity, and precipitation trends in arid and semiarid regions of Iran. *Arab J Geosci* 4:907–914
- Lee C-H, Chen W-P, Lee R-H (2006) Estimation of groundwater recharge using water balance coupled with base-flow-record estimation and stable base-flow analysis. *Environ Geol* 51:73–82
- Loáiciga HA (2009) Long-term climatic change and sustainable ground water resources management. *Environ Res Lett* 4:035004
- Mall R, Gupta A, Singh R, Singh R, Rathore L (2006) Water resources and climate change: an Indian perspective. *Curr Sci* 90:1610–1626
- Mandal S, Breach PA, Simonovic SP (2016) Uncertainty in precipitation projection under changing climate conditions: a regional case study. *Am J Clim Chang* 5:116
- Mariotti A, Zeng N, Yoon J-H, Artale V, Navarra A, Alpert P, Li LZ (2008) Mediterranean water cycle changes: transition to drier 21st century conditions in observations and CMIP3 simulations. *Environ Res Lett* 3:044001
- McKee TB, Doesken NJ, Kleist J The relationship of drought frequency and duration to time scales. In: *Proceedings of the 8th Conference on Applied Climatology*, 1993. vol 22. American Meteorological Society Boston, MA, pp 179–183
- Meigh J, Tate E, Mc Cartney M (2002) *Methods for identifying and monitoring river flow drought in Southern Africa* International Association of Hydrological Sciences, Publication:181–188
- Mirdashtvan M, Najafinejad A, Malekian A, Sa'doddin A (2018) Downscaling the contribution to uncertainty in climate-change assessments: representative concentration pathway (RCP) scenarios for the South Alborz Range. *Iran Meteorological Applications* 25: 414–422
- Modarres R, Sarhadi A, Burn DH (2016) Changes of extreme drought and flood events in Iran. *Global and Planetary Change* 144:67–81
- Modarres R, Ghadami M, Naderi S, Naderi M (2018) Future extreme rainfall change projections in the north of Iran. *Meteorological Applications* 25:40–48
- Motiee H, McBean E, Motiee AR, Majdzadeh Tabatabaei MR (2019) Assessment of climate change under CMIP5-RCP scenarios on downstream rivers glaciers–Sardabrud River of Alam-Kuh glacier, Iran. *International Journal of River Basin Management*:1–9
- Naderi M (2020) Assessment of water security under climate change for the large watershed of Dorudzan dam in southern Iran. *Hydrogeol J* 28:1553–1574. <https://doi.org/10.1007/s10040-020-02159-1>
- Naderi M, Raeisi E (2016) Climate change in a region with altitude differences and with precipitation from various sources. *South-Central Iran Theoretical and applied climatology* 124:529–540

- Naderi M, Saatsaz M (2019) Impact of climate change on the hydrology and water salinity in the Anzali wetland, northern Iran. *Hydrological Sciences Journal*
- O’Gorman PA (2015) Precipitation extremes under climate change. *Current Climate Change Reports* 1:49–59
- O’Gorman PA, Schneider T (2009) The physical basis for increases in precipitation extremes in simulations of 21st-century climate change. *Proceedings of the National Academy of Sciences* 106:14773–14777
- Pachauri RK et al. (2014) Climate change 2014: synthesis report. Contribution of working groups I, II and III to the fifth assessment report of the Intergovernmental Panel on Climate Change. IPCC, Paris
- Parab Consulting Engineers (1996) The primary study of hydrology in watershed of Salman Farsi Dam, part 2: climatology studies Fars Regional Water Authority, Iran
- Racsko P, Szeidl L, Semenov M (1991) A serial approach to local stochastic weather models. *Ecological modelling* 57:27–41
- Rahmani MA, Zarghami M (2013) A new approach to combine climate change projections by ordered weighting averaging operator; applications to northwestern provinces of Iran. *Global and Planetary Change* 102:41–50
- Raje D, Mujumdar P (2010) Hydrologic drought prediction under climate change: uncertainty modeling with Dempster–Shafer and Bayesian approaches. *Advances in Water Resources* 33:1176–1186
- Raziei T, Bordi I, Pereira L, Sutera A (2010) Space-time variability of hydrological drought and wetness in Iran using NCEP/NCAR and GPCC datasets. *Hydrol Earth Syst Sci* 14:1919–1930
- Raziei T, Bordi I, Pereira LS (2013) Regional drought modes in Iran using the SPI: the effect of time scale and spatial resolution. *Water Resour Manag* 27:1661–1674
- Reichler T, Kim J (2008) How well do coupled models simulate today’s climate? *Bull Am Meteorol Soc* 89:303–311
- Roshan G, Ghanghermeh A, Nasrabadi T, Meimandi JB (2013) Effect of global warming on intensity and frequency curves of precipitation, case study of northwestern Iran. *Water Resour Manag* 27:1563–1579
- Roshani A, Parak F, Hejazizade Z, Ghaemi H (2013) Studying the moisture flux over south and southwest of Iran: a case study from December 10 to 13, 1995 rain storm. *Earth Science Research* 2:34
- Scibek J, Allen DM, Cannon AJ, Whitfield PH (2007) Groundwater–surface water interaction under scenarios of climate change using a high-resolution transient groundwater model. *J Hydrol* 333:165–181
- Senior C, Mitchell J (1993) Carbon dioxide and climate. The impact of cloud parameterization. *J Clim* 6:393–418
- Semenov MA (2007) Development of high-resolution UKCIP02-based climate change scenarios in the UK. *Agricultural and Forest Meteorology* 144:127–138
- Semenov MA, Barrow EM (2002) A stochastic weather generator for use in climate impact studies. User manual. Hertfordshire, UK
- Semenov MA, Stratonovitch P (2010) Use of multi-model ensembles from global climate models for assessment of climate change impacts. *Clim Res* 41:1–14
- Semenov MA, Stratonovitch P (2015) Adapting wheat ideotypes for climate change: accounting for uncertainties in CMIP5 climate projections. *Clim Res* 65:123–139
- Semenov MA, Brooks RJ, Barrow EM, Richardson CW (1998) Comparison of the WGEN and LARS-WG stochastic weather generators for diverse climates. *Clim Res* 10:95–107
- Shatanawi K, Rahbeh M, Shatanawi M (2013) Characterizing, monitoring and forecasting of drought in Jordan River basin. *J Water Resource Prot* 5:1192
- Siler N, Roe G (2014) How will orographic precipitation respond to surface warming? An idealized thermodynamic perspective. *Geophysical Research Letters* 41:2606–2613
- Singh V, Goyal MK (2016) Analysis and trends of precipitation lapse rate and extreme indices over North Sikkim eastern Himalayas under CMIP5ESM-2M RCPs experiments. *Atmos Res* 167:34–60
- Solomon S et al (2007) Contribution of working group I to the fourth assessment report of the intergovernmental panel on climate change, 2007. Cambridge University Press, Cambridge
- Soltani M et al (2016) Assessment of climate variations in temperature and precipitation extreme events over Iran. *Theoretical and Applied Climatology* 126:775–795
- Spinoni J, Naumann G, Carrao H, Barbosa P, Vogt J (2014) World drought frequency, duration, and severity for 1951–2010. *Int J Climatol* 34:2792–2804
- Swain S, Hayhoe K (2015) CMIP5 projected changes in spring and summer drought and wet conditions over North America. *Climate Dynamics* 44:2737–2750
- Tabari H, Talaei PH (2011) Temporal variability of precipitation over Iran: 1966–2005. *J Hydrol* 396:313–320
- Task Group on Data Scenario Support for Impact and Climate Analysis TGICA (2007) Integrating analysis of regional climate change and response options. Intergovernmental Panel on Climate Change
- Thom HC (1958) A note on the gamma distribution. *Mon Weather Rev* 86:117–122
- Thompson JR, Crawley A, Kingston DG (2017) Future river flows and flood extent in the Upper Niger and Inner Niger Delta: GCM-related uncertainty using the CMIP5 ensemble. *Hydrological Sciences Journal* 62:2239–2265
- Tsakiris G, Vangelis H (2004) Towards a drought watch system based on spatial SPI. *Water Resour Manag* 18:1–12
- Ulbrich U, May W, Li L, Lionello P, Pinto JG, Somot S (2006) The Mediterranean climate change under global warming. In: *Developments in earth and environmental sciences*, vol 4. Elsevier, pp 399–415
- Vaghefi SA, Keykhai M, Jahanbakhshi F, Sheikholeslami J, Ahmadi A, Yang H, Abbaspour KC (2019) The future of extreme climate in Iran. *Scientific Reports* 9:1464
- Wada Y, van Beek LP, van Kempen CM, Reckman JW, Vasak S, Bierkens MF (2010) Global depletion of groundwater resources. *Geophys Res Lett* 37
- Wilby RL, Charles S, Zorita E, Timbal B, Whetton P, Mearns L (2004) Guidelines for use of climate scenarios developed from statistical downscaling methods. Supporting material of the Intergovernmental Panel on Climate Change. Available from the DDC of IPCC
- Woldeamlak S, Batelaan O, De Smedt F (2007) Effects of climate change on the groundwater system in the Grote-Nete catchment, Belgium. *Hydrogeol J* 15:891–901
- World Climate Research Programme (2018) CMIP5-DKRZ. <https://doi.org/10.1016/j.jhydrol.2011.05.002>

Publisher’s note Springer Nature remains neutral with regard to jurisdictional claims in published maps and institutional affiliations.